Managing for ecological surprises in metapopulations

Supplemental materials: Model details & results

Kyle L. Wilson[a]*, Alex Sawyer[a], Anna Potapova[a], Colin J. Bailey[a], Elissa Sweeney-Bergen[a],
Emma E. Hodgson[a], Kara J. Pitman[a], Karl Seitz[a], Lauren Law[a], Luke Warkentin[a],
Samantha M. Wilson[a], William I. Atlas[a], Daniella LoScerbo[b], Douglas C. Braun[c], Matthew
R. Sloat[d], M. Tim Tinker[e], and Jonathan W. Moore[a,b]

[a]Earth to Ocean Research Group, Simon Fraser University
[b]Resource and Environmental Management, Simon Fraser University
[c]Fisheries and Oceans Canada
[d]Wild Salmon Center
[e]Ecology and Evolutionary Biology, University of California Santa Cruz

05 September 2019

Contents

---

*Corresponding author - email: kl_wilson@sfu.ca

1

Metapopulation model

Local & metapopulation dynamics

Our metapopulation is defined by a set of local populations N_p for a species with a one year generation time with time-dynamics that follows birth (i.e., recruitment R), immigration, death, and emigration (BIDE) processes typical to metapopulation theory (Hanski 1998):

$$N_{it+1} = R_{it}\epsilon_{it} + I_{it} - D_{it} - E_{it} \tag{1}$$

where N_{it+1} is the number of adults in patch i at time t, R_{it} is number of recruits, I_{it} is number of recruits immigrating into patch i from any other patch, D_{it} is number of recruits that die due to disturbance regime, E_{it} is the number of recruits emigrating from patch i into any other patch, and ϵ_{it} is stochasticity in recruitment.

Resoure monitoring often occurs at the scale of the metapopulation (Anderson et al. 2015), hence we define metapopulation adults as:

$$MN_t = \sum_{i=1}^{N_p} N_{it} \tag{2}$$

with metapopulation recruits:

$$MR_t = \sum_{i=1}^{N_p} R_{it} \tag{3}$$

Local patch recruitment at time t depended on adult densities at *t-1* and followed a reparameterized Beverton-Holt function:

$$R_{it} = \frac{\alpha_i N_{it-1}}{1 + \dfrac{\alpha_i - 1}{\beta_i} N_{it-1}} \tag{4}$$

where α_i is the recruitment compensation ratio and β_i is local patch carrying capacity.

Management often monitors metapopulation resources as the aggregate of all local populations. For example, take a two patch metapopulation model that varies α_i and β_i parameters where:

```
alpha <- c(2, 4)
beta <- c(100, 200)
```

Here, recruitment compensation from local patches α_i gets averaged across the metapopulation leading to an average compensation ratio $\bar{\alpha}$ of 3. Likewise, the total carrying capacity of the metapopulation $\bar{\beta}$ becomes the summation of local patch carrying capacities $\sum \beta_i$, which is 300. This scale of monitoring generates the following local patch and metapopulation dynamics:
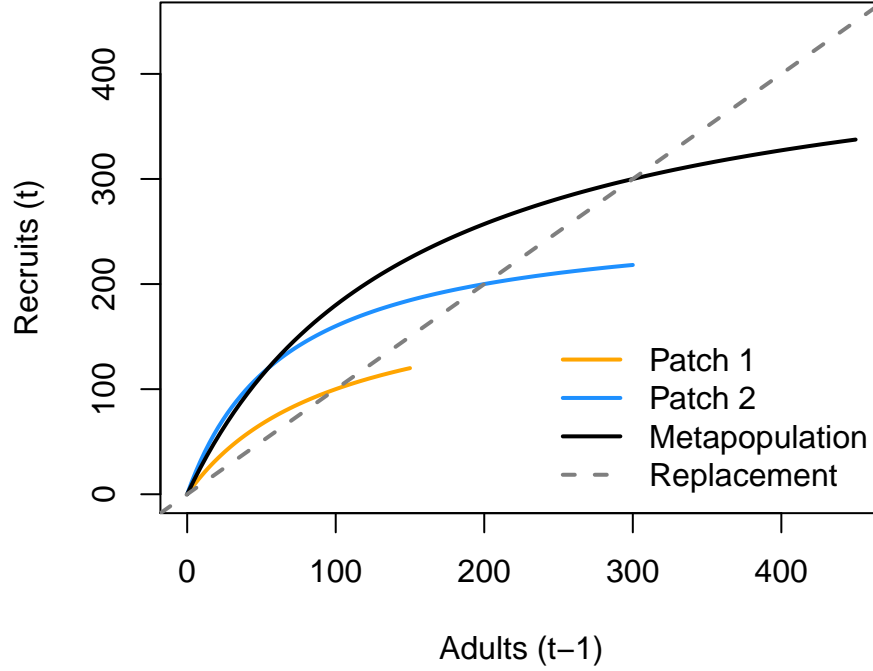
Figure S1: Metapopulation and local patch recruitment dynamics.

Creating the spatial networks

The next aspect to our metapopulation model is connecting the set of patches to one another (Yeakel et al. 2014). We need to specify the number of patches, their arrangements (i.e., connections), and how far apart they are from one another. We followed some classic metapopulation and source-sink arrangements to create four networks that generalize across a few real-world topologies: a linear habitat network (e.g., coastline), a dendritic or branching network (e.g., coastal rivers), a star network (e.g., mountain & valley, or lake with inlet tributaries), and a complex network (e.g., grasslands).

To make networks comparable, each spatial network type needs the same leading parameters (e.g., number of patches N_p and mean distance between neighboring patches $\bar{d}$). In this case, we set N_p to `16` and $\bar{d}$ to `1` unit (distance units are arbitrary). We used the `igraph` package (Csardi & Nepusz 2006) and some custom code to arrange our spatial networks as the following:
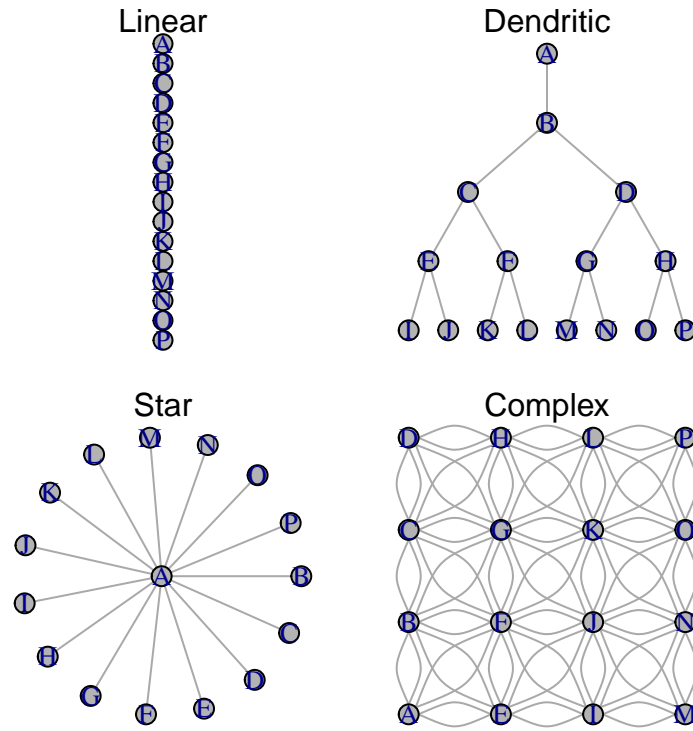
Figure S2: Four spatial network topologies.

65   Note that distances between neighbor patches in the above networks are equal.

66 An example dispersal matrix for the complex network:

```
67  ##   A B E F C G D H I J K L M N O P
68  ## A 0 1 1 1 2 2 3 3 2 2 2 3 3 3 3 3
69  ## B 1 0 1 1 1 1 2 2 2 2 2 2 3 3 3 3
70  ## E 1 1 0 1 2 2 3 3 1 1 2 3 2 2 2 3
71  ## F 1 1 1 0 1 1 2 2 1 1 1 2 2 2 2 2
72  ## C 2 1 2 1 0 1 1 1 2 2 2 2 3 3 3 3
73  ## G 2 1 2 1 1 0 1 1 2 1 1 1 2 2 2 2
74  ## D 3 2 3 2 1 1 0 1 3 2 2 2 3 3 3 3
75  ## H 3 2 3 2 1 1 1 0 3 2 1 1 3 2 2 2
76  ## I 2 2 1 1 2 2 3 3 0 1 2 3 1 1 2 3
77  ## J 2 2 1 1 2 1 2 2 1 0 1 2 1 1 1 2
78  ## K 2 2 2 1 2 1 2 1 2 1 0 1 2 1 1 1
79  ## L 3 2 3 2 2 1 2 1 3 2 1 0 3 2 1 1
80  ## M 3 3 2 2 3 2 3 3 1 1 2 3 0 1 2 3
81  ## N 3 3 2 2 3 2 3 2 1 1 1 2 1 0 1 2
82  ## O 3 3 2 2 3 2 3 2 2 1 1 1 2 1 0 1
83  ## P 3 3 3 2 3 2 3 2 3 2 1 1 3 2 1 0
```

84 **Dispersal**

85 Dispersal from patch i into patch j depends on constant dispersal rate ω (defined as the proportion of total
86 local recruits that will disperse) and an exponential distance-decay function between i and j with distance
87 cost to dispersal m following Anderson et al. (2015):

$$E_{ij(t)} = \omega R_{it} p_{ij} \tag{5}$$

88 where E_{ij} is the total dispersing animals from patch i into patch j resulting from dispersal rate ω, total
89 number of local recruits R_{it}, and probability of dispersal between patches p_{ij}:

$$p_{ij} = \frac{e^{-md_{ij}}}{\sum\limits_{\substack{j=1 \\ j \neq i}}^{N_p} e^{-md_{ij}}} \tag{6}$$

90 where d_{ij} is the pairwise distance between patches, m is the distance cost to dispersal. The summation term
91 in the denominator normalizes the probability of moving to any patch to between 0 and 1 with the constraint
92 that dispersers cannot move back into their home patch (i.e., $j \neq i$. With $\bar{d} = 1$, $m = 0.5$, $\omega = 0.1$, $R_{it} = 100$
93 in a linear network:
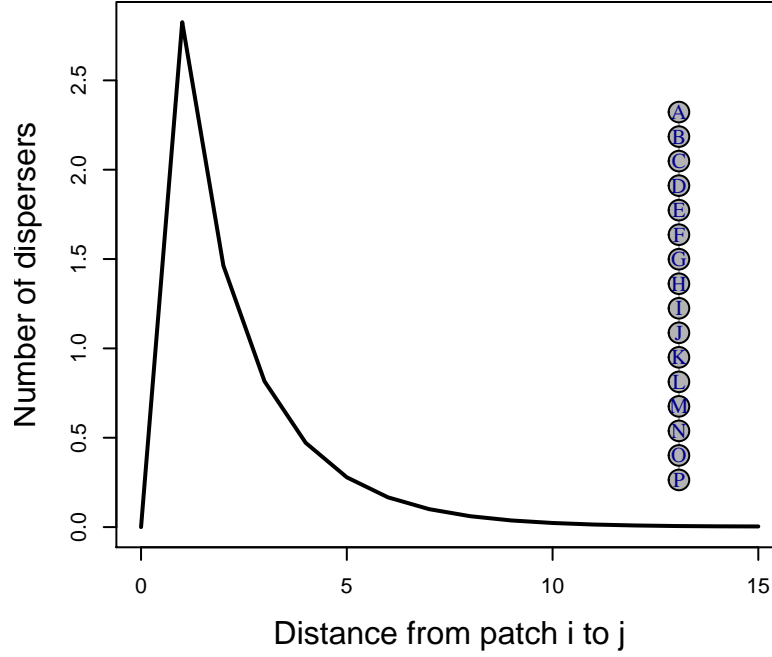
Figure S3: Example dispersal patterns across linear network.

Disturbance regimes

In all scenarios, disturbance was applied after 50 years of equilibrating the metapopulaton at pristine conditions. At year 51, we applied the disturbance regime (the regime varied from *uniform, localized, random,* and *localized, extirpation* - see *Scenarios* below). Disturbance immediately removes a set proportion of the metapopulation adults at that time (i.e., 0.9 of $MN_{t=51}$). Once applied, the metapopulation was no longer disturbed and spatio-temporal recovery dynamics emerged naturally from these new conditions.
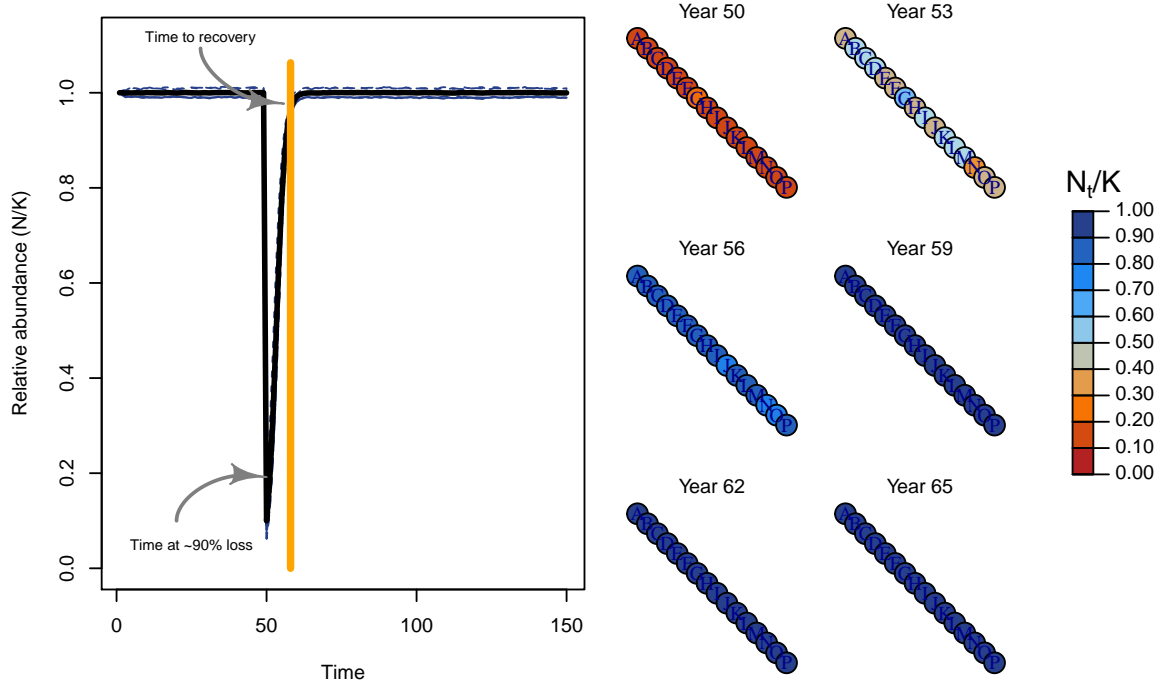
Figure S4: Recovery regime of metapopulation with linear topology through time (left) and space (right).

Recruitment stochasticity

Our model allowed for stochastic recruitment that followed a lognormal distribution with average variation in recruitment of σ_R. In cases of stochastic recruitment, the expected recruitment:

$$R_{it} = \frac{\alpha_i N_{it-1}}{1 + \dfrac{\alpha_i - 1}{\beta_i} N_{it-1}} \tag{7}$$

becomes:

$$R_{it} = \frac{\alpha_i N_{it-1}}{1 + \dfrac{\alpha_i - 1}{\beta_i} N_{it-1}} e^{\left(\epsilon_{it} - \frac{ln(\sigma_R^2 + 1)}{2}\right)} \tag{8}$$

where lognormal deviates for each patch i at time t are drawn from a multivariate normal distribution (MVN) If σ_R is low, then metapopulation dynamics approach the deterministic case. In some scenarios, we evaluate the role of spatially and/or temporally correlated deviates across the metapopulations to model potential common drivers affecting metapopulation dynamics (e.g., Moran effects). Expected recruitment deviates followed a first-order autoregression model such that:

$$\epsilon_{it} = \rho_T \epsilon_{t-1} + MVN(\mu = 0, \Sigma = \sigma_R(1 - \rho_T^2)e^{(-\rho_S D_{ij})}) \tag{9}$$

₁₀₉ where ρ_T is temporal correlation (bounded $0-1$) ρ_S is rate of distance-decay in spatial correlation (bounded
₁₁₀ $0-\infty$ with higher values leading to independent patches). If rho_T is 0 and rho_S is high, then annual
₁₁₁ recruitment deviates are independent. We illustrate the effects of four kinds of recruitment deviates below
₁₁₂ using the same random number generator seed:
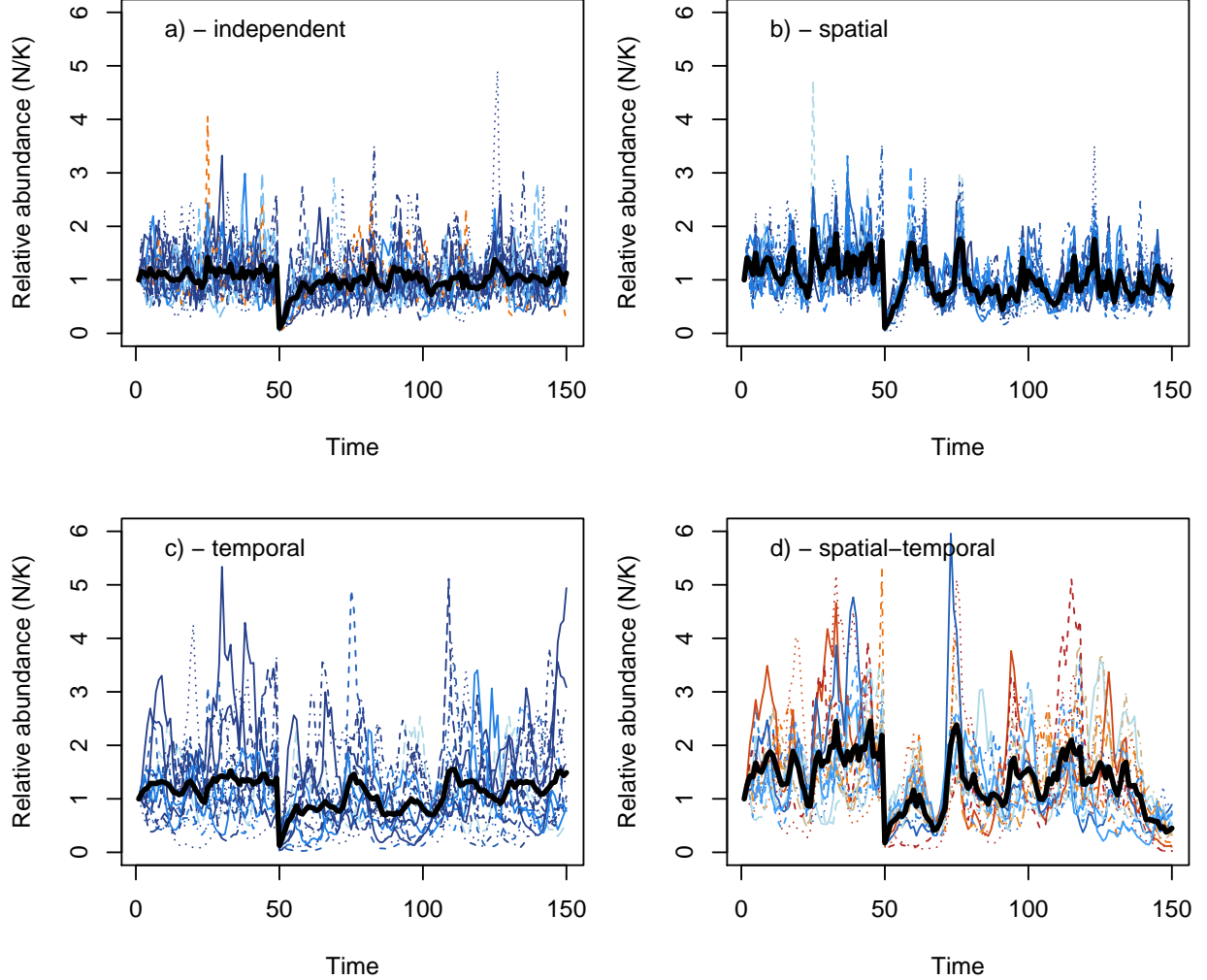
Figure S5: Metapopulation dynamics with independent (a), spatially correlated (b), temporally correlated
(c), and spatio-temporally correlated (d) recruitment deviates.

Post-disturbance outcomes

₁₁₃

₁₁₄ We measured the following post-disturbance outcomes to track the temporal and spatial recovery regime of
₁₁₅ the metapopulation.

₁₁₆ 1. Collapse (a) & recovery rate (b) after disturbance:

₁₁₇   a. Collapse rate is defined as the number of simulations where metapopulation abundance failed to
₁₁₈   recover to `1.0` of the average pre-disturbance abundance for `5` consecutive years post-disturbance.
₁₁₉   This "collapse rate" reflects the risk of a long-term state shift in metapopulation dynamics after
₁₂₀   disturbance in the face of stochasticity.
₁₂₁   b. Recovery rate the number of years to average pre-disturbance abundance for `5` consecutive years.

¹²² The recovery rate (either in the number of generations or in the rate of recovery per year)
¹²³ captures how quickly the aggregate metapopulation recovers from disturbance but doesn't take
¹²⁴ into account whether any given local patches recover to their pre-disturbance capacity.

¹²⁵ 2. Patch occupancy - the mean number of patches with `>0.1` local carrying capacity after disturbance in
¹²⁶ the short-term (5 years), medium-term (10 years), and long-term (25 years). This value characterizes
¹²⁷ the expected risk of spatial contractions or local patch collapses, and reflects how interactions between
¹²⁸ spatial structure, disturbance, and dispersal shape source-sink dynamics and the ability to provide (or
¹²⁹ not) rescue effects and recover local patches.

¹³⁰ 3. The ratio of expected maximum surplus production (we term MSY) to true maximum surplus
¹³¹ production summed across all patches from fitted stock-recruitment model to aggregate across
¹³² metapopulation such that:

$$\Delta_{MSY} = \frac{M\hat{S}Y_M}{\sum_{i=1}^{N_p} MSY_i} \tag{10}$$

¹³³ A value of 1.0 would indicate that the disturbed metapopulation can sustain itself against the same
¹³⁴ disturbance regime as the sum of each patch independently. In other words, is the metapopulation
¹³⁵ more than ($\Delta_{MSY}>1.0$), less than ($\Delta_{MSY}<1.0$), or equal to the sum of its parts ($\Delta_{MSY}=1.0$).

¹³⁶ **Monitoring & management at aggregate-scale**

¹³⁷ While true metapopulation dynamics are controlled by local patch dynamics and dispersal such that:

$$N_{it} = R_{it}\epsilon_{it} + I_{it} - D_{it} - E_{it} \tag{11}$$

$$R_{it} = \frac{\alpha_i N_{it-1}}{1 + \frac{\alpha_i - 1}{\beta_i}N_{it-1}} \tag{12}$$

$$MN_t = \sum_{i=1}^{N_p} N_{it} \tag{13}$$

$$MR_t = \sum_{i=1}^{N_p} R_{it} \tag{14}$$

¹³⁸ Natural resoure managers often monitors and manages at the scale of the metapopulation. Hence,
¹³⁹ management at this scale inherently defines the stock-recruitment dynamics of the aggregate complex of
¹⁴⁰ patches (i.e., metapopulation) as:

$$MR_t = \frac{\hat{\alpha}_t MN_{t-1}}{1 + \frac{\hat{\alpha}_t - 1}{\hat{\beta}_t}MN_{it-1}} \tag{15}$$

141 where $\hat{\alpha}_t$ is the estimated compensation ratio averaged across the metapopulation at time t and $\hat{\beta}_t$ is the
142 estimated carrying capacity of the entire metapopulation. Necessarily, these estimates emerge from
143 monitoring data collected across all patches and are sensitive to the quality of the data and how local patches
144 perform through time. For example, temporal shifts in productivity regimes may be masked if most of the
145 data were sampled before the regime shift. To help surmount these issues, modern resource assessments use
146 data weighting and penalties (i.e., priors) when fitting models to data.

147 In our assessment, we weighted recent years of sampling over more distant years such that:
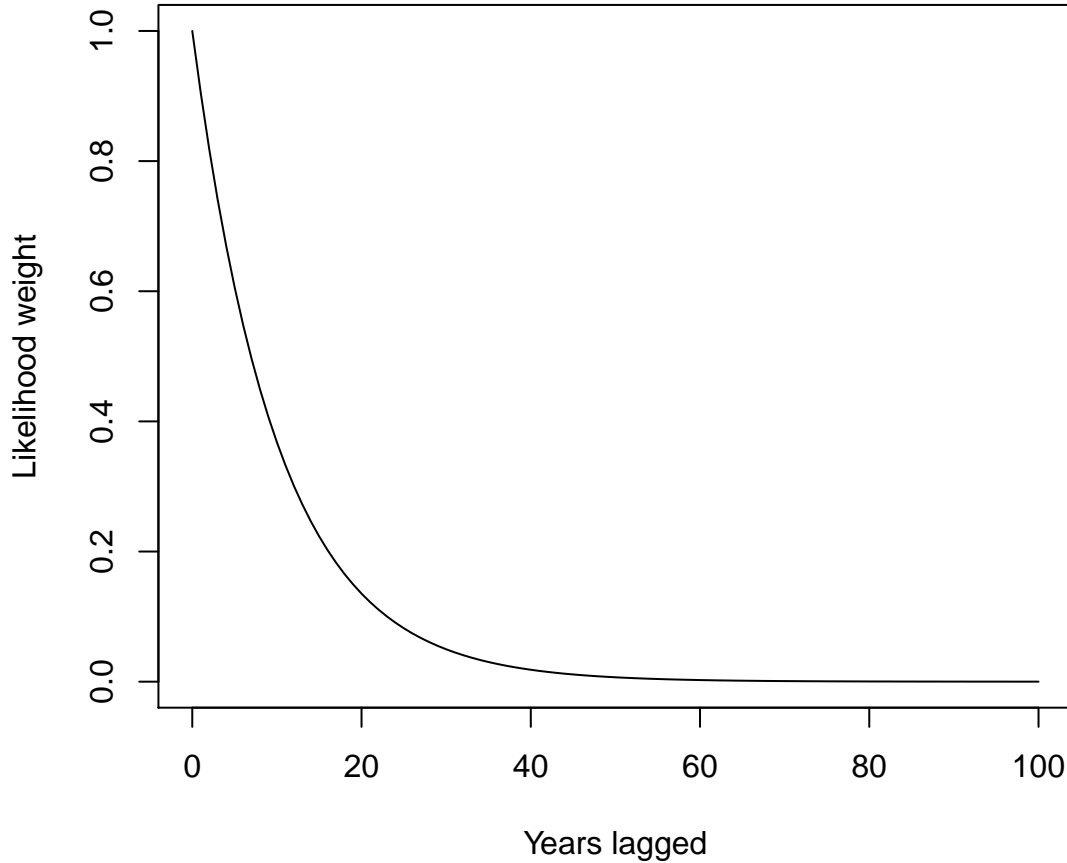

Figure S6: Likelihood weighting for samples collected over time from current year of sampling.

148 This forward-weighting approach increased the sensitivity of the monitoring sub-model to detect
149 demographic changes in the post-disturbance recovery regime. Data-weighting is increasingly being used in
150 resource monitoring, although how weights are developed and applied to data is a case-by-case basis.

151 Furthermore, we used penalized normal likelihoods on both $\hat{\alpha}_t$ and $\hat{\beta}_t$ such that:

$$\hat{\alpha}_t \sim N(\mu = \hat{\alpha_{t-1}}, \sigma = 3\hat{\alpha_{t-1}}) \tag{16}$$

10

152 and

$$\hat{\beta}_t \sim N(\mu = \hat{\beta_{t-1}}, \sigma = 3\hat{\beta_{t-1}}) \tag{17}$$

153 where $\mu = \hat{\alpha_{t-1}}$ and $\mu = \hat{\beta_{t-1}}$ represents the best estimates from the previous assessment and the 3 in the σ
154 term represents a 300% coefficient of variation. We used these penalized likelihoods to fit the above
155 aggregate stock-recruitment model with *lognormal* error to the metapopulation stock-recruit data collected
156 at time *t*. We used the following function and fitted to the below θ parameters (termed `theta` in the function
157 `optim()` using the `L-BFGS-B` optimizer with a lower bound on $\hat{\alpha}$ of `1.01` (i.e., constrained to be at least
158 above replacement).

```r
SRfn <- function(theta, data, lastYr) {
    a.hat <- theta[1]
    b.hat <- exp(theta[2])
    sd.hat <- exp(theta[3])
    rec.mean <- (a.hat * data$spawners)/(1 + ((a.hat - 1)/b.hat) * data$spawners)
    # negative log likelihood on recruitment parameters
    nll <- -1 * sum(dlnorm(data$recruits, meanlog = log(rec.mean), sdlog = sd.hat,
        log = TRUE) * data$weights, na.rm = TRUE)
    # penalized likelihood on estimated alpha
    penalty1 <- -dnorm(a.hat, lastYr$alphaLstYr, 4 * lastYr$alphaLstYr, log = TRUE)
    # penalized likelihood on estimated carrying capacity
    penalty2 <- -dnorm(b.hat, lastYr$metaKLstYr, 4 * lastYr$metaKLstYr, log = TRUE)
    jnll <- sum(c(nll, penalty1, penalty2), na.rm = TRUE)
    return(jnll)
}
```

159 This above function allows us to assess the bias in $\hat{\alpha}_t$, $\hat{\beta}_t$, and $\hat{MR}_t$ compared to true $\bar{\alpha}$, $\bar{\beta}$, and MR_t across
160 the metapopulation. This then allows us to see how much information management & monitoring programs
161 are missing when they assess metapopulations at the aggregate (rather than local) scales.

162 **Finding maximum sustainable yield**

163 Resource managers measure productivity with a variety of performance reference points (Forrest et al. 2010).
164 One of the most widely used metrics, commonly called *Maximum Sustainable Yield* in fisheries and other
165 harvest literature (MSY), relates to the largest loss the population can sustain over an indefinite period of
166 time while maximizing its ability to replenish itself. Under density-dependent growth, individuals' growth,
167 survival, and reproduction at low population densities are not constrained by limited resources, but overall
168 production is low because there are few individuals. At high densities, limited resources increasingly constrain
169 individual's reproductive success until the population reaches carrying capacity, and overall production drops
170 to zero because per-capita success is low. However, at some intermediate densities, both per-capita and
171 overall production is high, and population growth is at its maximum point due to the large number of
172 reproducing individuals. At this point, there is the maximum surplus of individuals produced above
173 replacement that can help to withstand disturbance or harvest regimes and contribute to future recovery,
174 either through increasing local patch densities or by emigrating neighboring patches providing "rescue effects".

175 Under Beverton-Holt or Ricker density-dependent recuitment, however, there exists no analytical solution for
176 calculating MSY. Therefore, we used numerical methods and a one dimensional root finder to iteratively
177 search for the population mortality that maximized surplus production in the metapopulation. We term this
178 mortality F_{MSY} and can use this mortality value to calculate maximum surplus production MSY, the adult
179 densities that produce MSY (termed N_{MSY}), and the recruits that result from this (termed R_{MSY}).

```r
# uniroot numerical search

yieldRoot <- function(alpha, beta, Fcur, model) {
```

```r
    Ucur <- 1 - exp(-Fcur)
    if (model == "Beverton-Holt") {
        # population model is R ~ (CR * S)/(1+(CR-1)/K * S): reparameterized
        # Beverton-Holt
        adults <- beta * exp(-Fcur)
        recruits <- (alpha * adults)/(1 + ((alpha - 1)/beta) * adults)
        yield <- recruits - adults
    }
    if (model == "Ricker") {
        # population model is R ~ CR * S * e(-log(CR)/K * S): reparameterized Ricker
        adults <- beta * exp(-Fcur)
        recruits <- alpha * adults * exp((-log(alpha)/beta) * adults)
        yield <- recruits - adults
    }
    return(list(recruits = recruits, adults = adults, yield = yield))
}


# Return approximate gradient for integral

fun_yield <- function(Fcur, alpha, beta, delta, model) {
    y1 <- yieldRoot(alpha = alpha, beta = beta, Fcur = Fcur - delta/2, model = model)$yield
    y2 <- yieldRoot(alpha = alpha, beta = beta, Fcur = Fcur + delta/2, model = model)$yield
    approx.gradient <- (y2 - y1)/delta
    return(approx.gradient)
}


# uniroot search for optimal yield and Fmsy
findMSY <- function(alpha, beta, Npatches, model) {
    F_msy <- NULL
    for (i in 1:Npatches) {
        a_p <- alpha[i]
        b_p <- beta[i]
        F_msy[i] <- uniroot(fun_yield, interval = c(0, 1), extendInt = "yes",
            alpha = a_p, beta = b_p, delta = 1e-04, model = model)$root
    }
    MSY <- sapply(1:Npatches, function(x) {
        yieldRoot(alpha = alpha[x], beta = beta[x], Fcur = F_msy[[x]][1], model = model)
    })
    return(list(F_msy = F_msy, MSY = MSY))
}
```

Scenarios

We tested all combinations of the following eight processes (below) and ran a 100 bootstraps per scenario to estimate the mean for each of the above outcomes.

1. Homogenous and spatially variable recruitment compensation ratio across patches, i.e. intrinsic rate of population growth (α_i).

2. Homogenous and spatially variable local carrying capacity across patches, i.e. asymptote of expected recruits at high adult densities (β_i)

3. Disturbances where a proportion of individuals removed from metapopulation (e.g., 0.90) occurs.

    a. *uniform* - random individuals removed at equal vulnerability across all patches.

₁₈₉   b. *localized, random* - random individuals removed from randomly selected subset of patches (as long
₁₉₀   as the target individuals lost in the metapopulation can be achieved in that subset of patches)
₁₉₁   c. *localized, extirpation* - total extirpation of randomly selected subset of patches (as long as the
₁₉₂   target individuals lost in the metapopulation can be achieved in that subset of patches)

₁₉₃ 4. Density-independent dispersal rates ω from 0 to 20% of individuals within a patch will disperse.

₁₉₄ 5. Topology of the spatial networks with linear, dendritic, star, and complex networks. Each network with
₁₉₅ N_p of 16 and distance between patches $\bar{d}$ of 1.

₁₉₆ 6. Stochastic recruitment deviates from low, medium, high coefficient of variation on lognormal error.
₁₉₇   Generate stochasticity in time-dynamics via random recruitement deviates away from expected.

₁₉₈ 7. Temporal correlation in recruitment deviates from low, medium, high correlation (i.e., good year at
₁₉₉   time *t* begets good year at time *t+1*).

₂₀₀ 8. Spatial correlation in recruitment deviates among patches from low, medium, to high correlation (i.e.,
₂₀₁   neighboring patches go up or down together).

Example results

₂₀₃ We demonstrate our metapopulation model with an example outcome for a linear network composed of 16
₂₀₄ patches, a dispersal rate of 0.01 and a high enough dispersal cost such that individuals are only willing to
₂₀₅ move to their closest neighboring patches. This limits the strength of potential rescue effects. For this
₂₀₆ example, patches varied in their productivity and carrying capacity but will have deterministic population
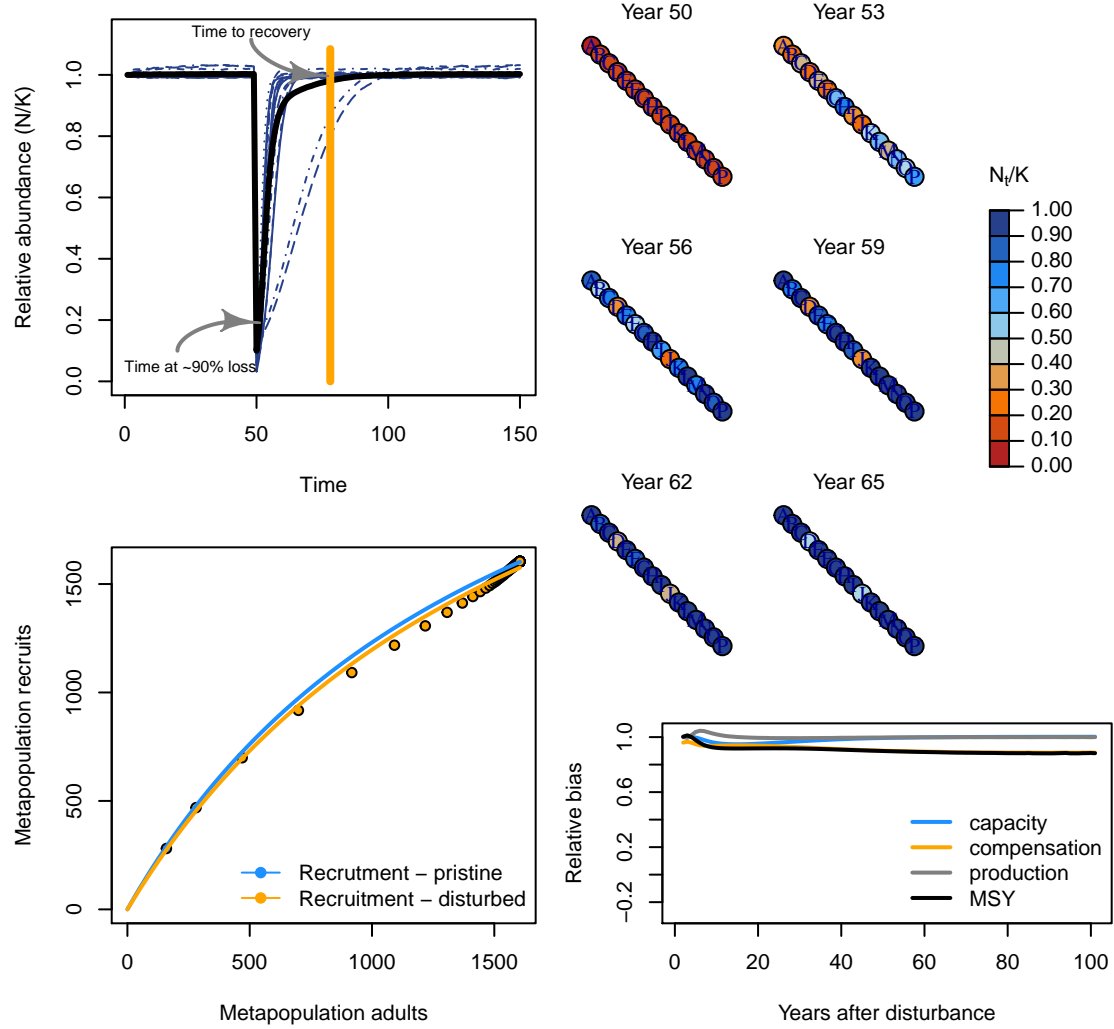₂₀₇ dynamics.

Figure S7: Spatial recovery regime of metapopulation with linear topology through time (top left) and space (top right). Recruitment dynamics before and 10 years after disturbance (bottom left). Relative bias in aggregate-scale estimates of carrying capacity, compensation ratio, and recruitment production in recovery phase (bottom right).

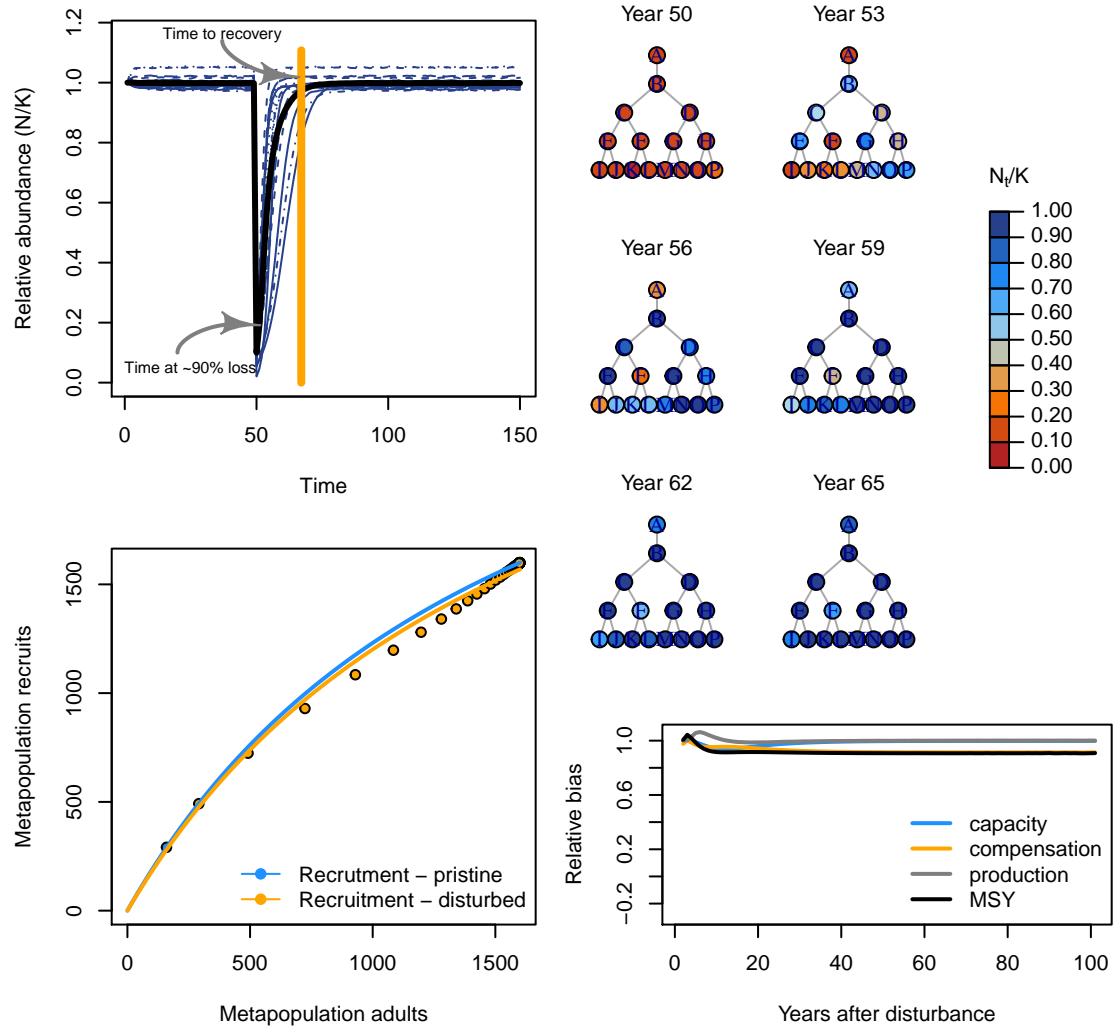208 We can then contrast this with a different network shape, like a dendritic network.

Figure S8: Spatial recovery regime of metapopulation with dendritic topology.

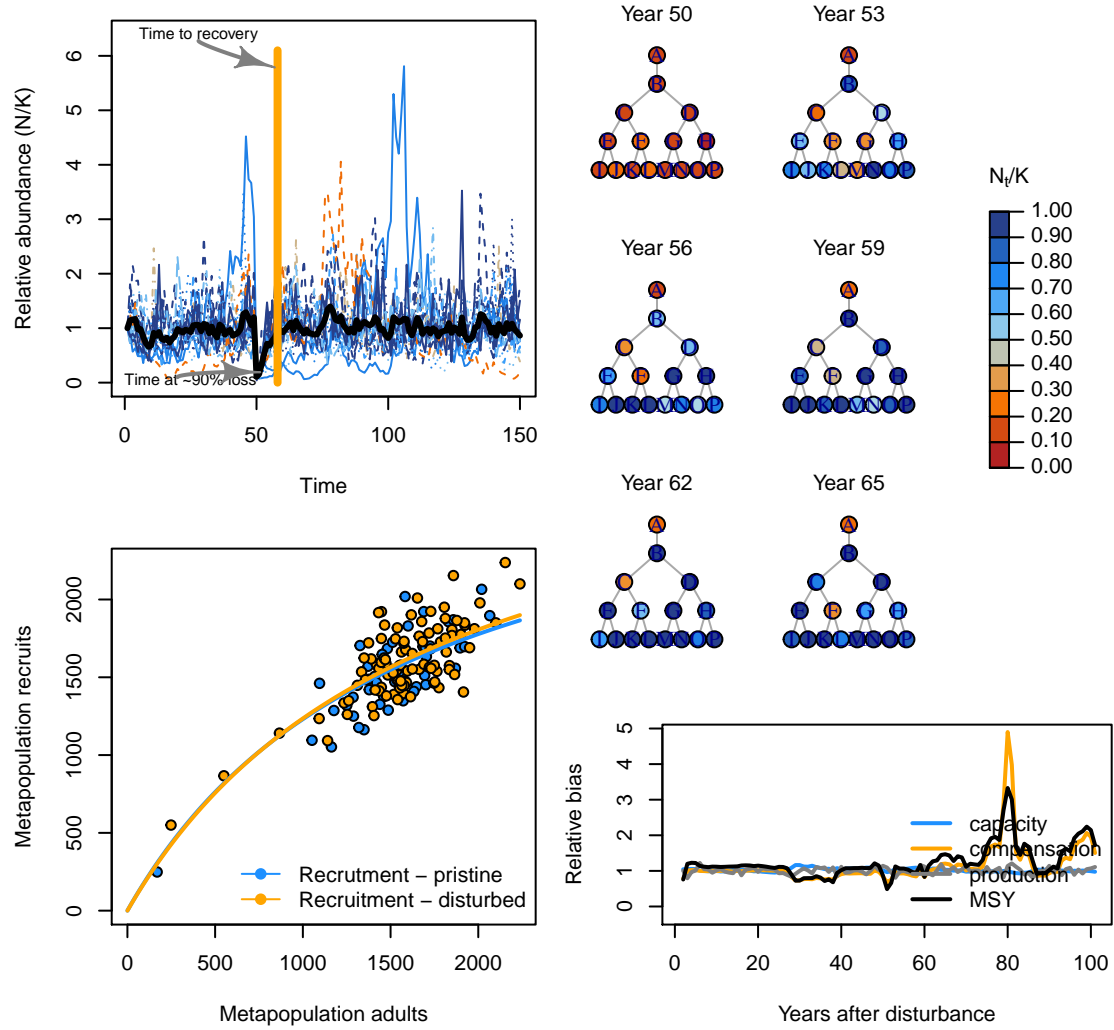209   Now, let's add some stochasticity to recruitment and see how this affects the recovery regime.

Figure S9: Spatial recovery regime of stochastic metapopulation.

210 Next, we can contrast with a disturbance regime where the disturbance is concentrated on local patches that
211 can be completely extirpated (rather than the disturbance being applied proportionally across all patches
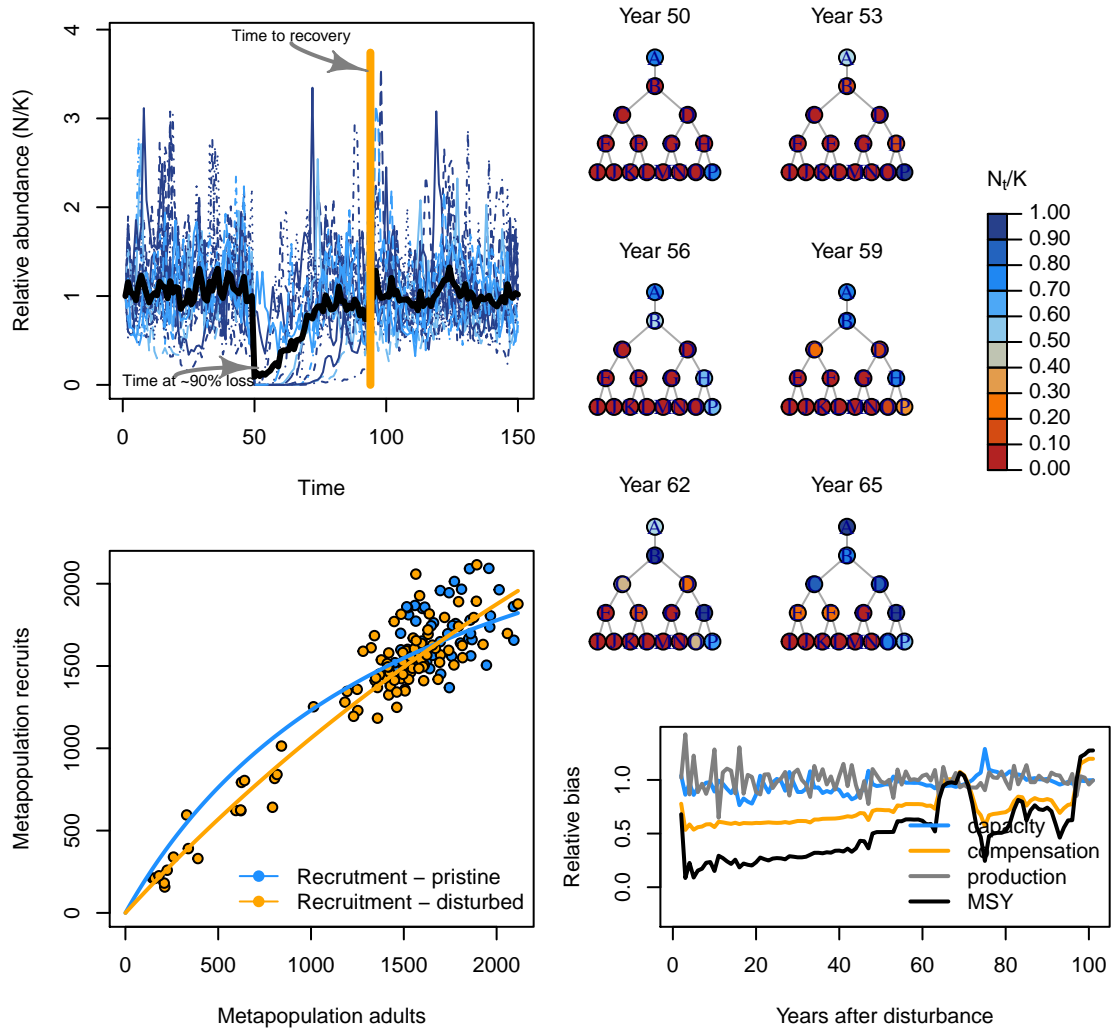212 e.g., a mixed-stock fishery).

Figure S10: Spatial recovery regime of stochastic metapopulation.

²¹³ **General patterns**

²¹⁴ **Effects of disturbance regime**
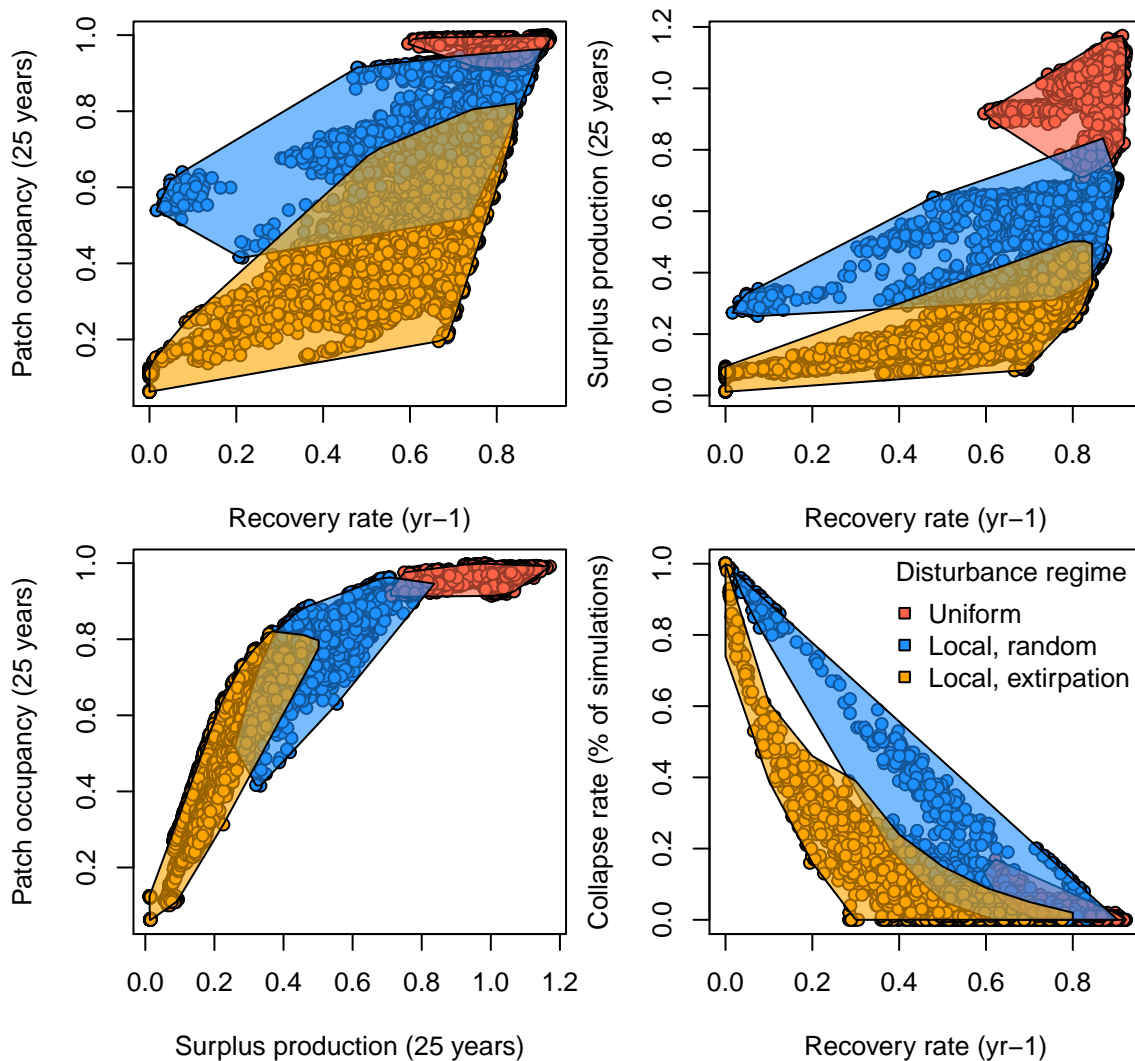

Figure S11: Spatial and temporal recovery patterns along disturbance regimes.

²¹⁵ **Role of network structure & dispersal**

²¹⁶ We now show some general patterns in how variable patch demographic rates, network structure, dispersal,
²¹⁷ disturbance, recruitment stochasticity, and spatio-temporal correlations variation affects metapopulation
²¹⁸ *recovery rates*, *maximum sustainable yield* (analogous to the maximum rate of loss the system can sustain),
²¹⁹ and *collapse rate* (i.e, the number of simulations where the metapopulation fails to recover), and *patch*
²²⁰ *occupancy* (i.e., number of patches with local abundance above some baseline).

²²¹ First, lets show recovery rates for a scenario where (1) patches have the same local productivities and
²²² carrying capacities, (2) patches have different productivities and carrying capacities, (3) recruitment is
²²³ deterministic and patches are different, and (4) spatial-temporal correlation in stochastic recruitment.

²²⁴ Below, we can see three main effects on recovery rates (number of generations to reach recovery). First,
²²⁵ recovery gets faster with increased dispersal. Most of the action here takes place at low rates of dispersal
²²⁶ indicating most spatial topologies don't need much dispersal to quicken their recovery. In preliminary runs,

227 dispersal rates of `0.05-0.2` provided similar recovery patterns. Second, more localized disturbances regimes
228 lead to slower recovery. Third, linearized networks have slower recovery times than interconnected, complex
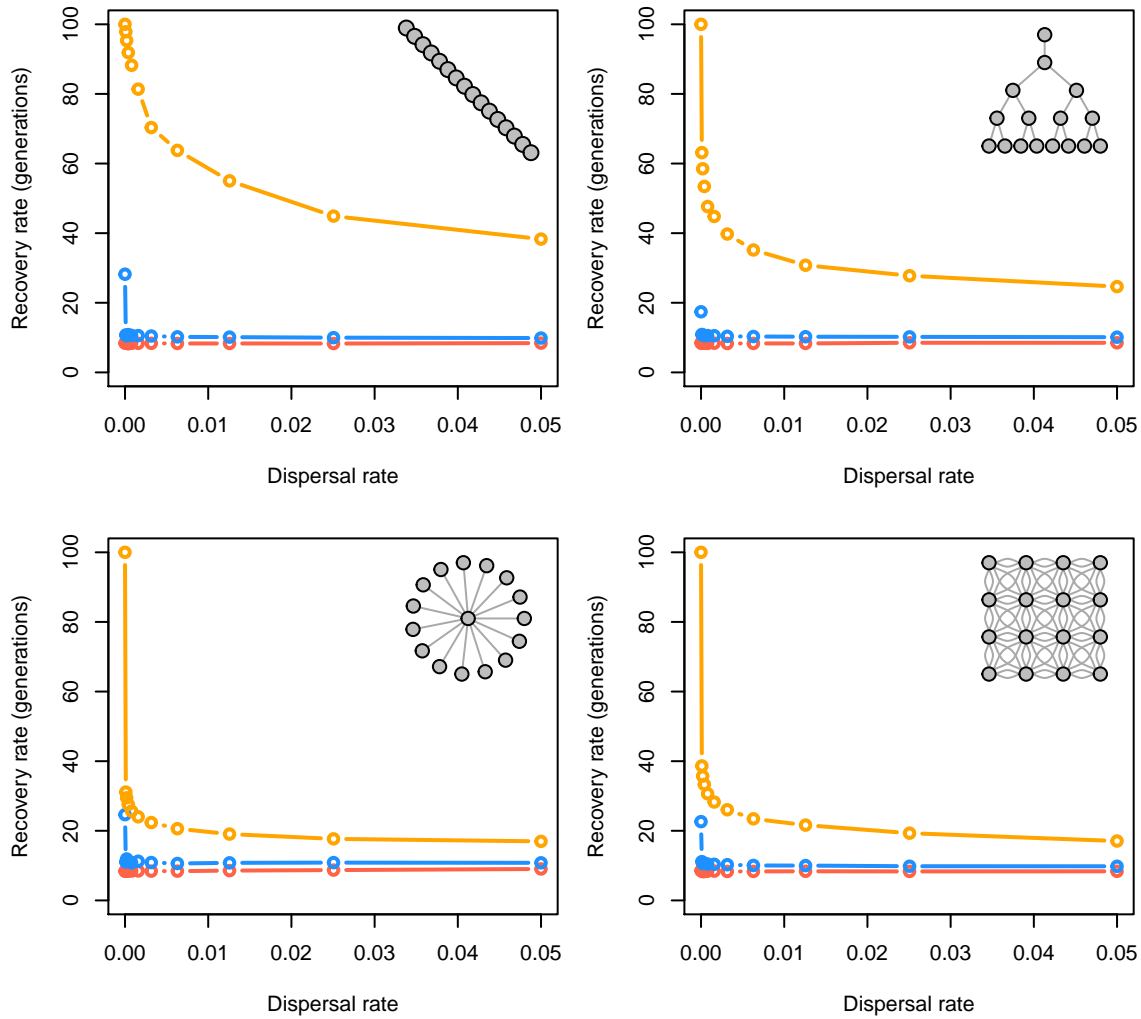229 networks suggesting that rescue effects take some time to cascade through the entire network of patches.
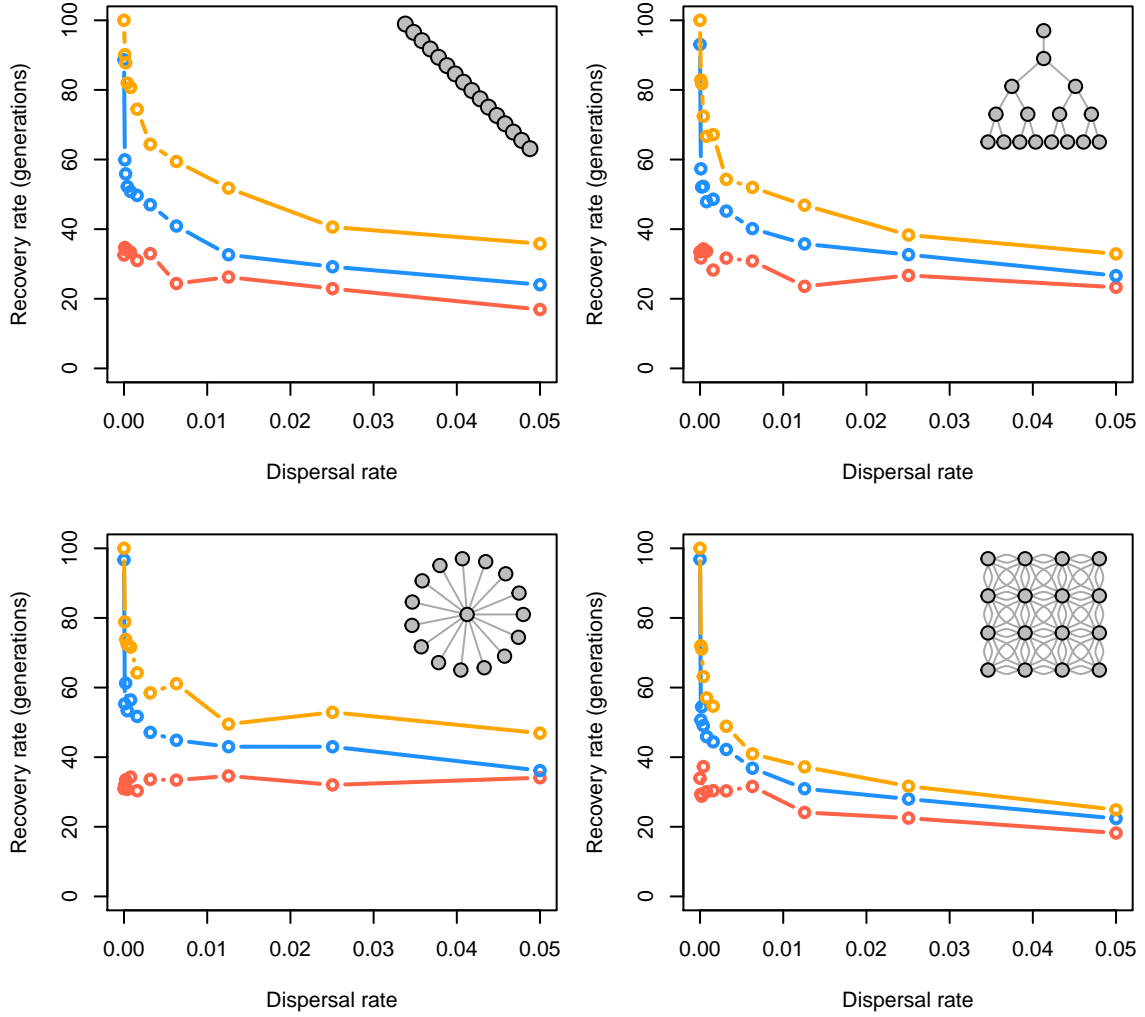

Figure S12: Recovery rates along dispersal, disturbance (red - uniform; blue - localized, random; orange - localized, extirpation), and network gradients without stochasticity.

₂₃₀ Now, lets show recovery rates for the same scenario with deterministic recruitment but allowing for patches to
₂₃₁ vary in productivity and carrying capacity. In addition to the same three main effects of dispersal, network,
₂₃₂ and disturbance noted above, we also see variable patch productivities slows recovery across all scenarios.
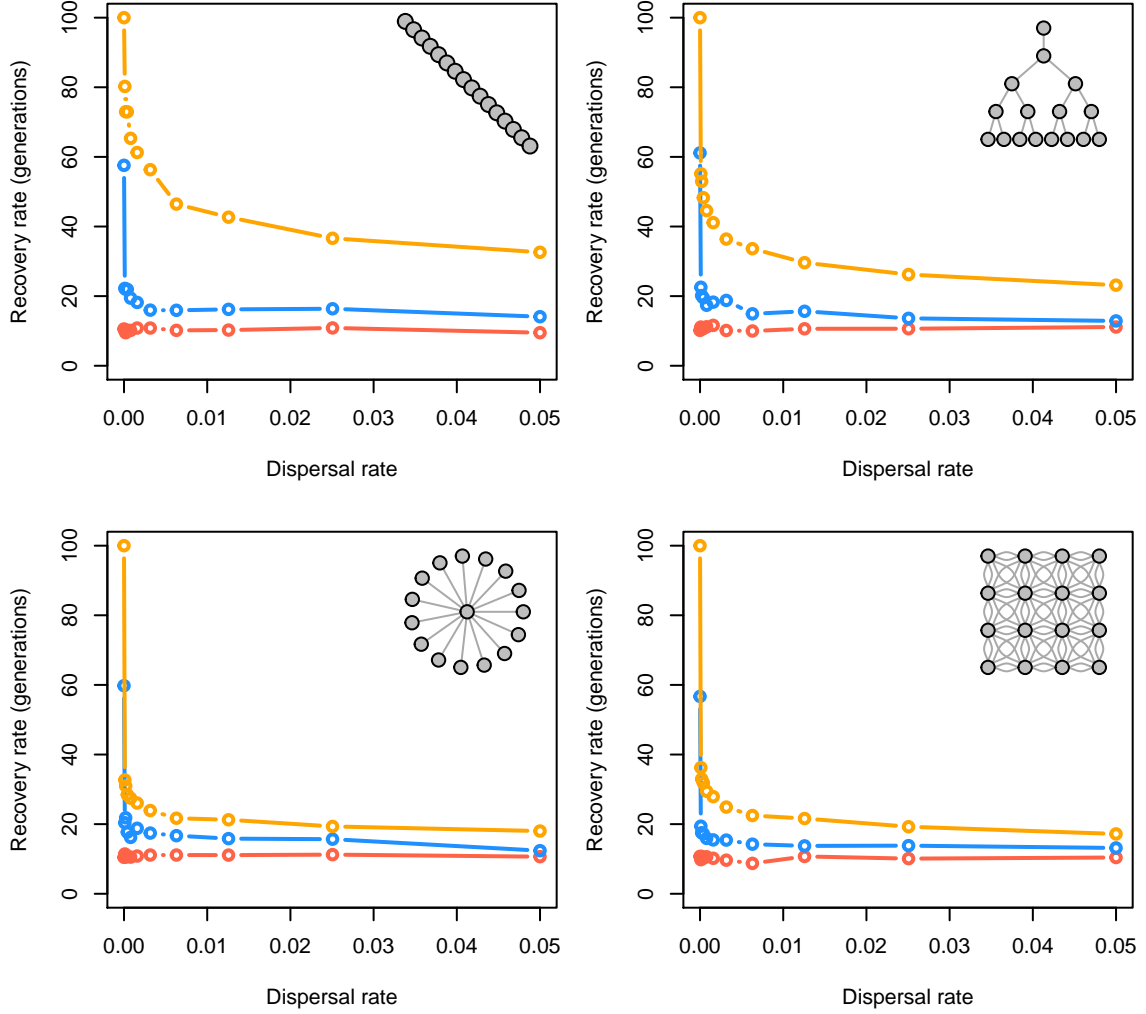

Figure S13: Recovery rates along dispersal, disturbance (red - uniform; blue - localized, random; orange - localized, extirpation), and network gradients with variable local productivity and carrying capacities.

₂₃₃ Now, lets show recovery rates for the same scenario but allowing for recruitment to be stochastic (but
₂₃₄ patches are the same in demography). We see the same three main effects of dispersal, network, and
₂₃₅ disturbance noted above. We also see a few subtle changes: (1) stochasticity slows recovery for uniform and
₂₃₆ local disturbance, but (2) quickens recovery for extreme local disturbance.
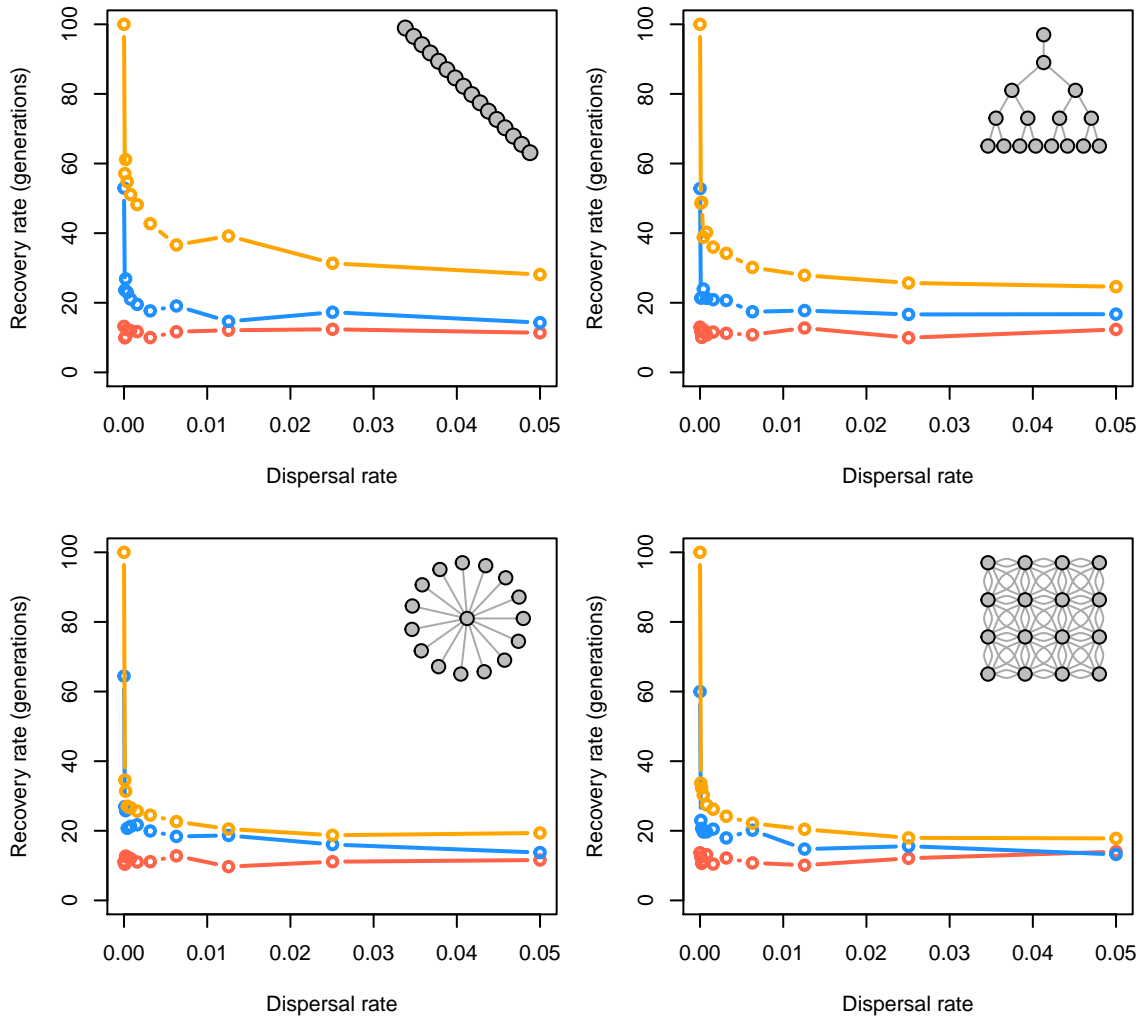

Figure S14: Recovery rates along dispersal, disturbance (red - uniform; blue - localized, random; orange - localized, extirpation), and network gradients with stochasticity.

²³⁷ Now, lets show recovery rates for the same scenarios but with spatial and temporal correlations in recruitment
²³⁸ stochasticity. In addition to the same effects of stochasticity, we also generally see a small effect of slower
²³⁹ recovery times for uniform and local disturbance, but faster recovery times for extreme localized disturbance.

Figure S15: Recovery rates along dispersal, disturbance (red - uniform; blue - localized, random; orange - localized, extirpation), and network gradients with high spatial-temporal correlation in recruitment variation.

240 **General patterns in MSY**

241 **MSY with deterministic recruitment where patches are the same**

242 We now show similar patterns in how the maximum surplus production of the whole metapopulation (i.e.,
243 MSY) shifts in the first 25 years post-disturbance compared to the sum of MSY for each patch. A value of
244 1.0 would indicate that the disturbed metapopulation can sustain itself against the same disturbance regime
245 as the sum of each patch independently. In other words, is the metapopulation more, less, or equal to the
246 sum of its parts.

247 We will show 25-year MSY patterns for a scenario where (1) patches have the same local productivities and
248 carrying capacities, (2) patches have different productivities and carrying capacities, (3) recruitment is
249 deterministic and patches are different, (4) spatial-temporal correlation in stochastic recruitment.

250 Below, we can see three main effects on recovery rates (number of generations to reach recovery). First,
251 recovery gets faster with increased dispersal. Most of the action here takes place at low rates of dispersal
252 indicating most spatial topologies don't need much dispersal to quicken their recovery. In preliminary runs,
253 dispersal rates of `0.05-0.2` provided similar recovery patterns. Second, more localized disturbances regimes
254 lead to slower recovery. Third, linearized networks have slower recovery times than interconnected, complex
255 networks suggesting that rescue effects take some time to cascade through the entire network of patches.
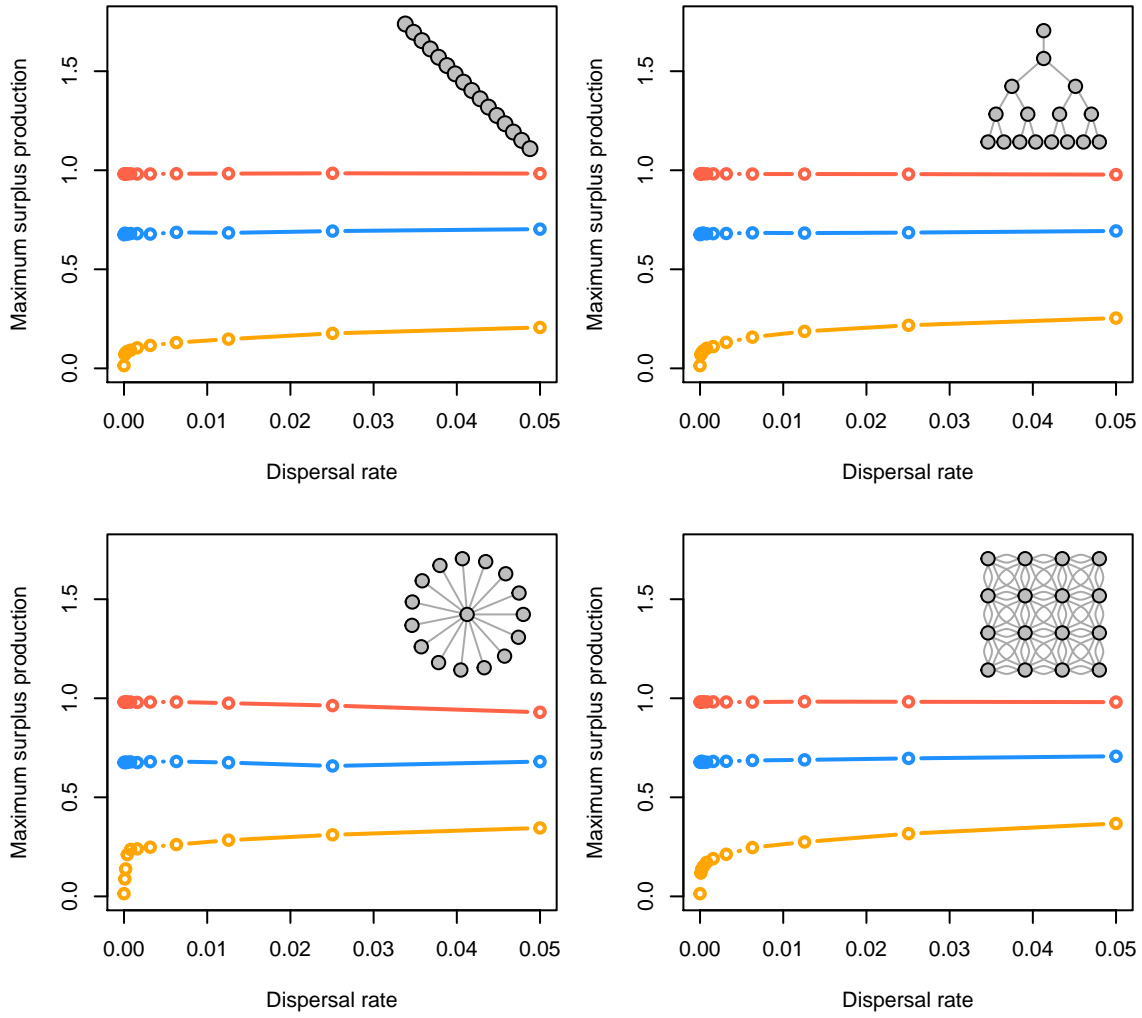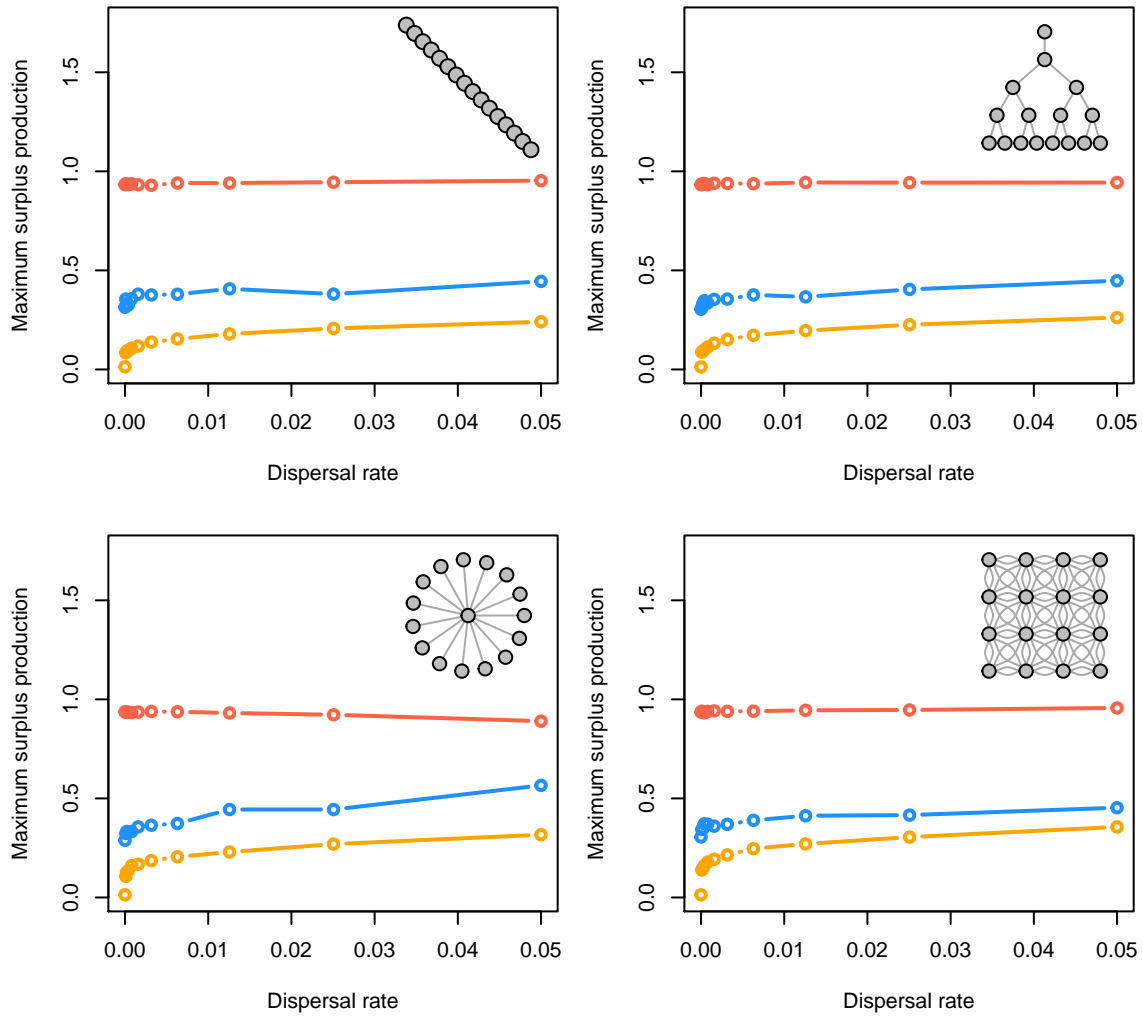
Figure S16: Maximum surplus production along dispersal, disturbance (red - uniform; blue - localized, random; orange - localized, extirpation), and network gradients with deterministic recruitment and the same patches.

₂₅₆ **MSY with variable patches**

₂₅₇ Now, we illustrate how variable patch demography affects the 25-year average MSY.
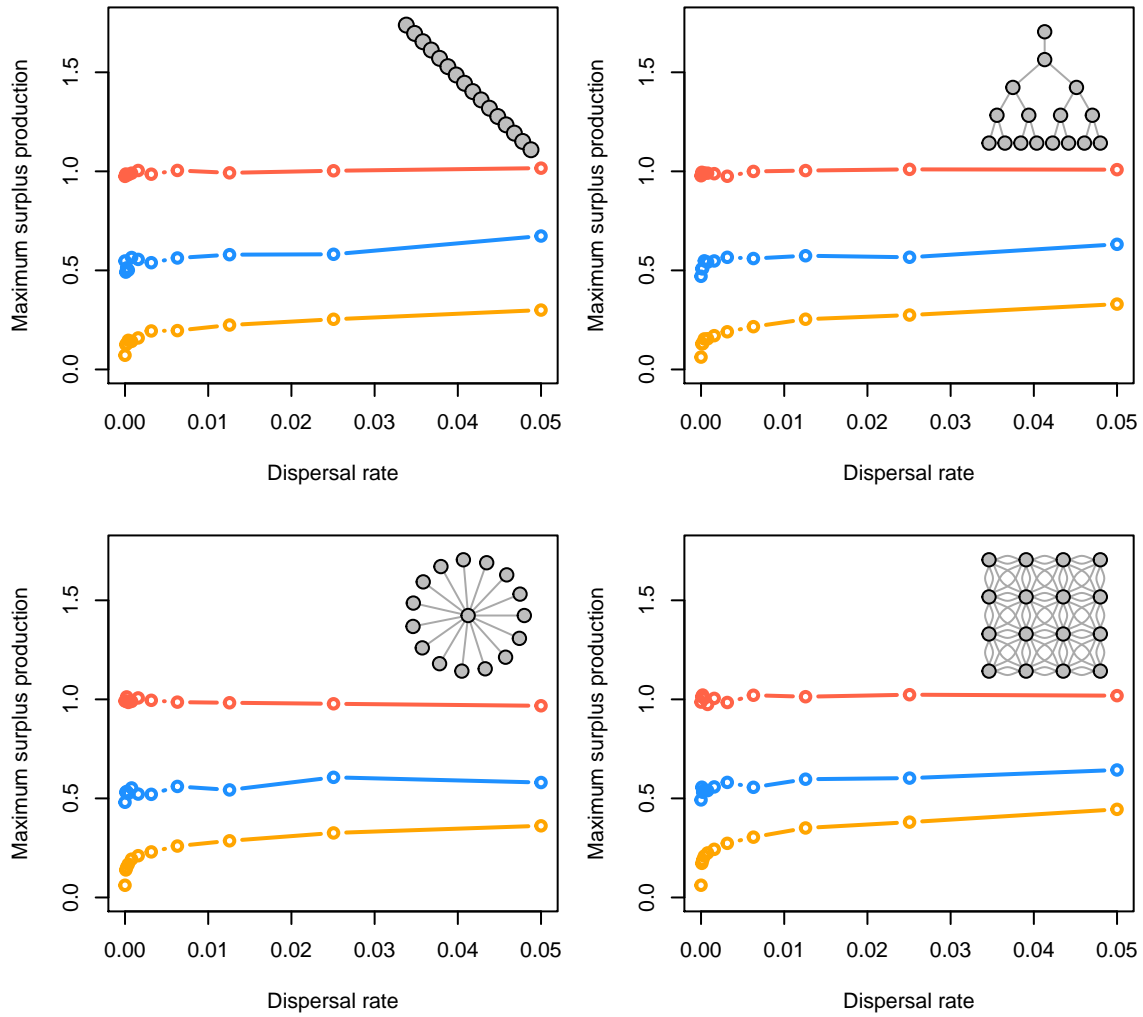

Figure S17: Maximum surplus production along dispersal, disturbance (red - uniform; blue - localized, random; orange - localized, extirpation), and network gradients with variable patches.

25

258   MSY with variable patches and stochasticity

259   Now, we illustrate how variable patch demography affects the 25-year average MSY.
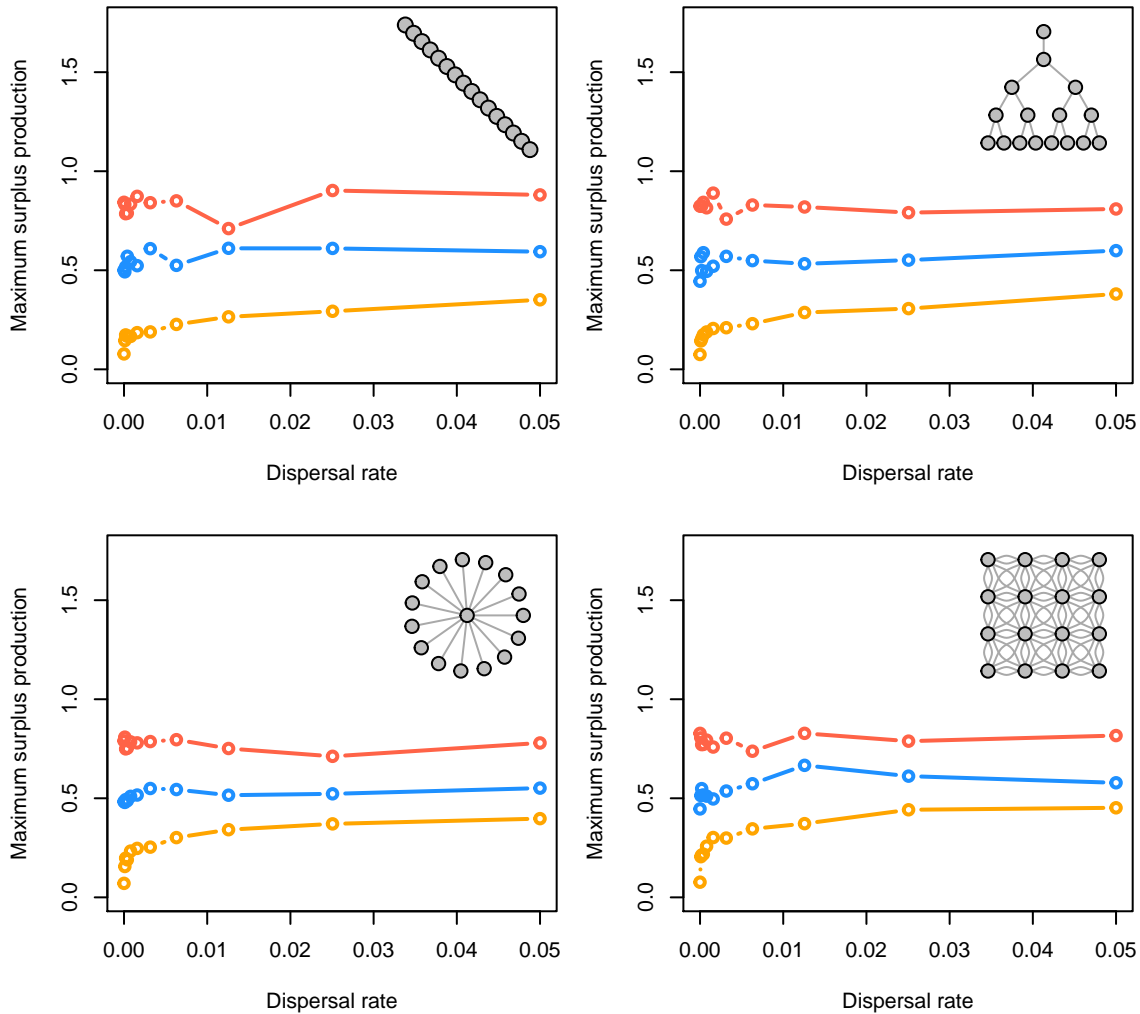

Figure S18: Maximum surplus production along dispersal, disturbance (red - uniform; blue - localized, random; orange - localized, extirpation), and network gradients with variable patches and stochasticity.

²⁶⁰ **MSY with variable patches, and spatio-temporally correlated stochasticity**

²⁶¹ Now, we illustrate how variable patch demography and high spatial-temporal correlations in stochastic
²⁶² recruitment affects the 25-year average MSY.

Figure S19: Maximum surplus production along dispersal, disturbance (red - uniform; blue - localized, random; orange - localized, extirpation), and network gradients with high spatial-temporal correlation in recruitment stochasticity and variable patches.

General patterns in the risk of hysteresis & state shifts

We now show similar patterns in the rate of long-term collapse across the metapopulation after 100 generations post-disturbance. Collapse rate % is defined as the number of simulations where metapopulation abundance failed to reach at least `1.0` of the average pre-disturbance abundance for `5` consecutive years after disturbance. This "collapse rate" reflects the risk of a long-term state shift in metapopulation dynamics after disturbance in the face of stochasticity. We start with a scenario with deterministic recruitment where patches are the same.
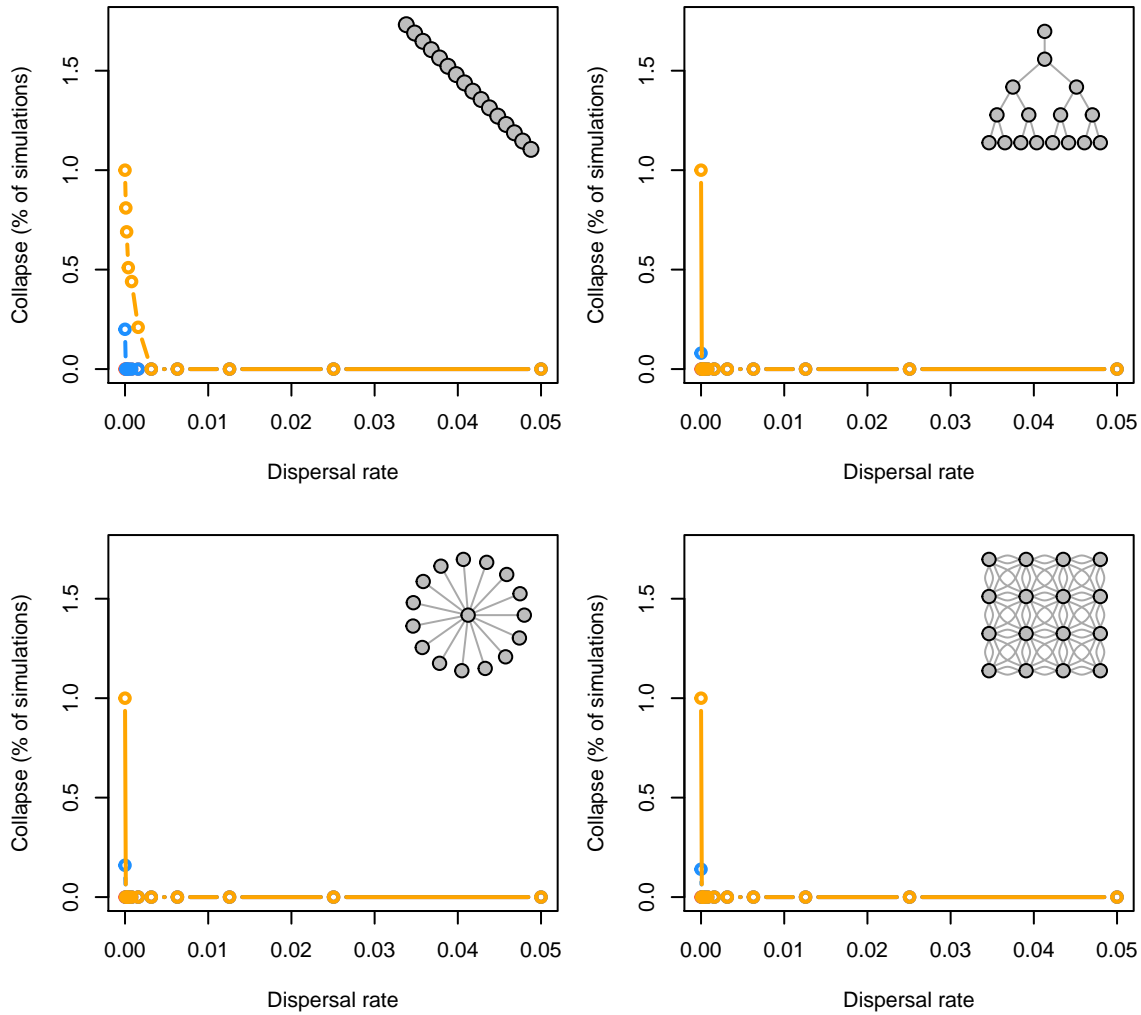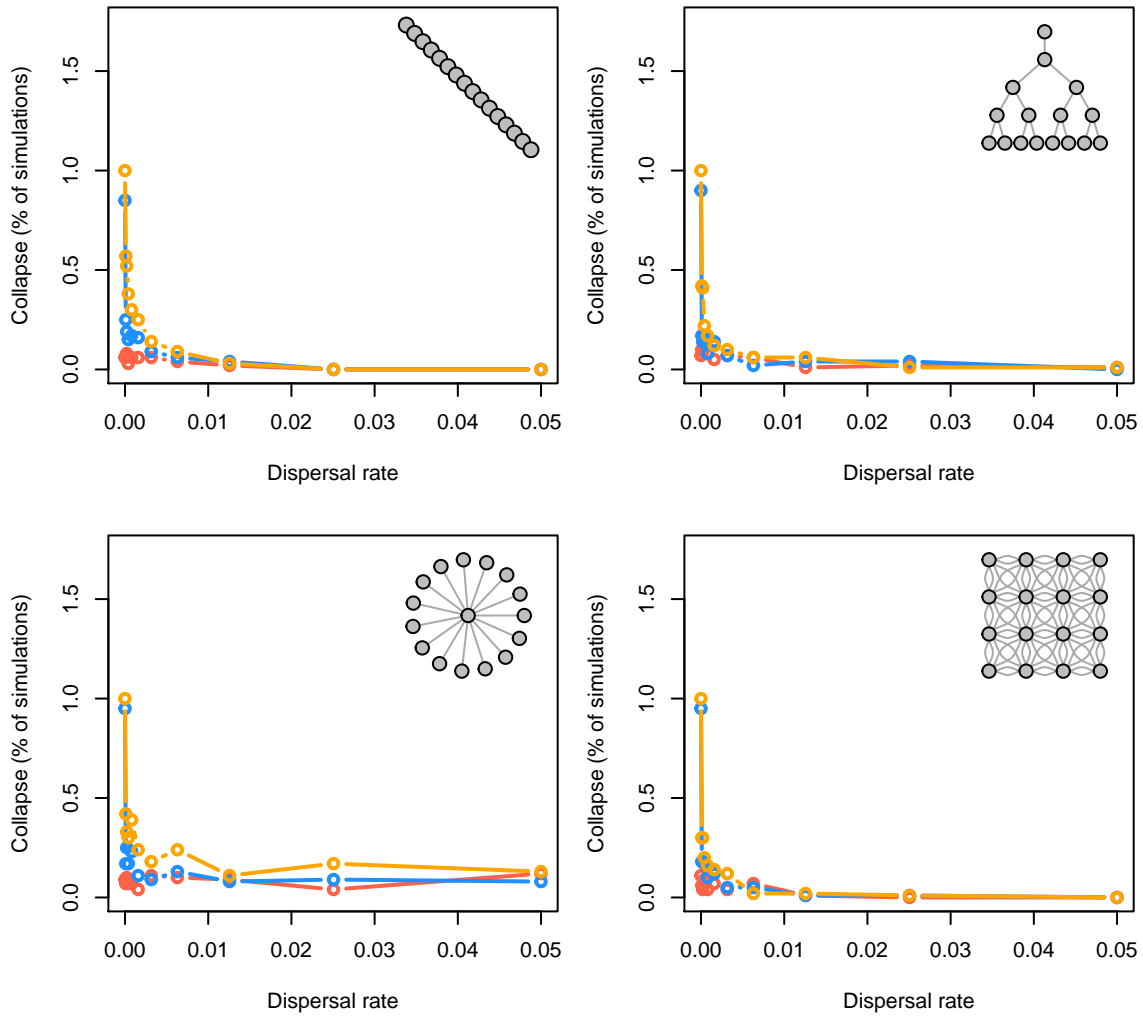

Figure S20: Risk of state shift after 100 generations along dispersal, disturbance (red - uniform; blue - localized, random; orange - localized, extirpation), and network gradients with high spatial-temporal correlation in recruitment variation.

₂₇₀ **State shifts with variable patches**

₂₇₁ Now, we illustrate how variable patch demography affects the risk of a state shift.
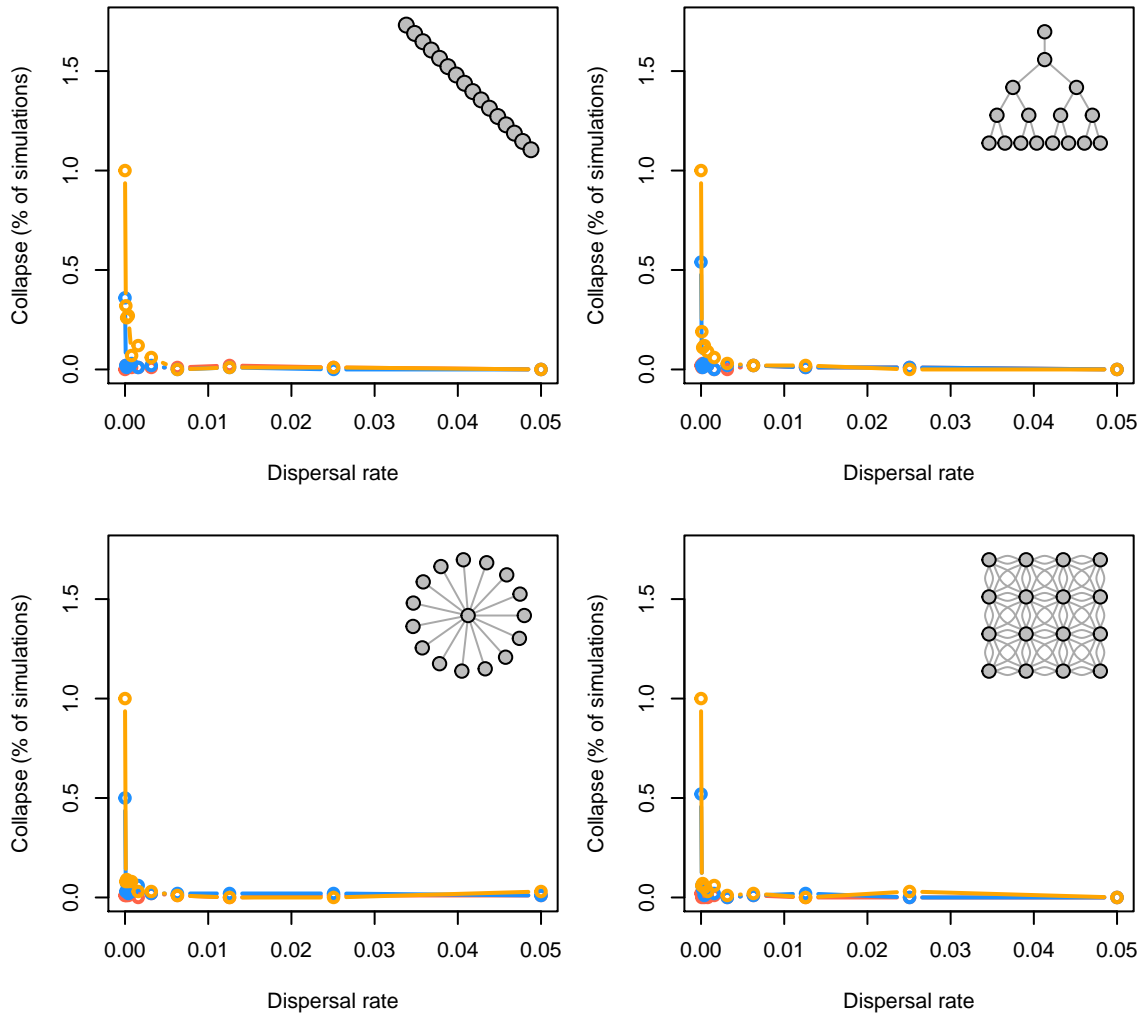

Figure S21: Risk of state shift after 100 generations along dispersal, disturbance (red - uniform; blue - localized, random; orange - localized, extirpation), and network gradients with variable patches.

²⁷² **State shifts with variable patches and stochasticity**

²⁷³ Now, we illustrate how variable patch demography and stochastic recruitment affects the risk of state shift.

Figure S22: Risk of state shift after 100 generations along dispersal, disturbance (red - uniform; blue - localized, random; orange - localized, extirpation), and network gradients with variable patches and stochastic recruitment.

₂₇₄ **State shifts with variable patches, and spatio-temporally correlated stochasticity**

₂₇₅ Now, we illustrate how variable patch demography and high spatial-temporal correlations in stochastic
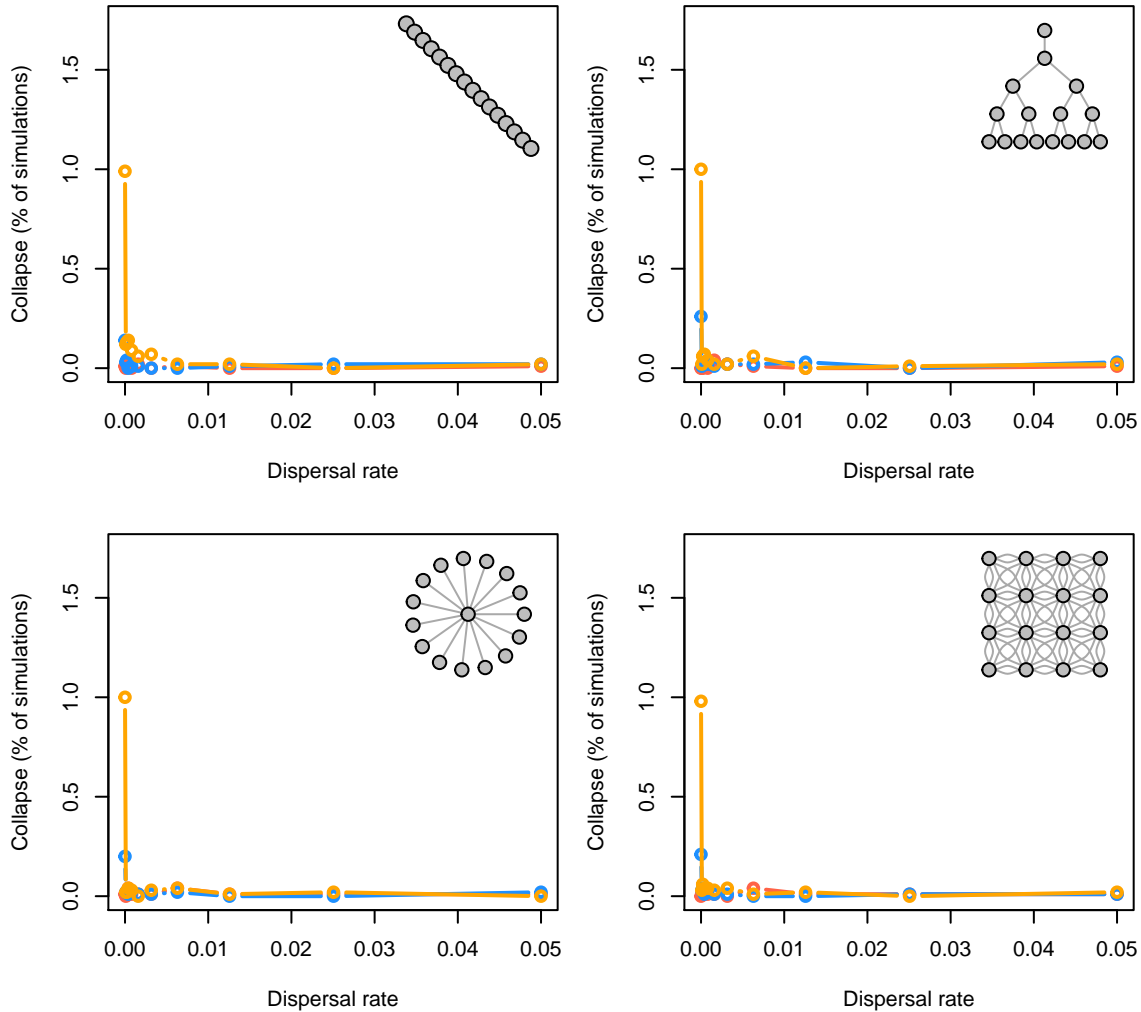₂₇₆ recruitment affects the risk of a state shift.

Figure S23: Risk of state shift (lack of recovery or spatial contraction) after 100 generations along dispersal, disturbance (red - uniform; blue - localized, random; orange - localized, extirpation), and network gradients with variable patches, and spatial-temporal correlations in stochastic recruitment.

31

General patterns in the risk of spatial contraction

We now show similar patterns in patch occupancy after 25 years post-disturbance. Patch occupancy is defined as the average number of patches that fail to recover above `0.1` pre-disturbance abundance for scenario with deterministic recruitment where patches are the same. Patch occupancy characterizes the expected risk of spatial contractions or local patch collapses, and reflects how interactions between spatial structure, disturbance, and dispersal affect source-sink dynamics and the provisioning of rescue effects to local patches.
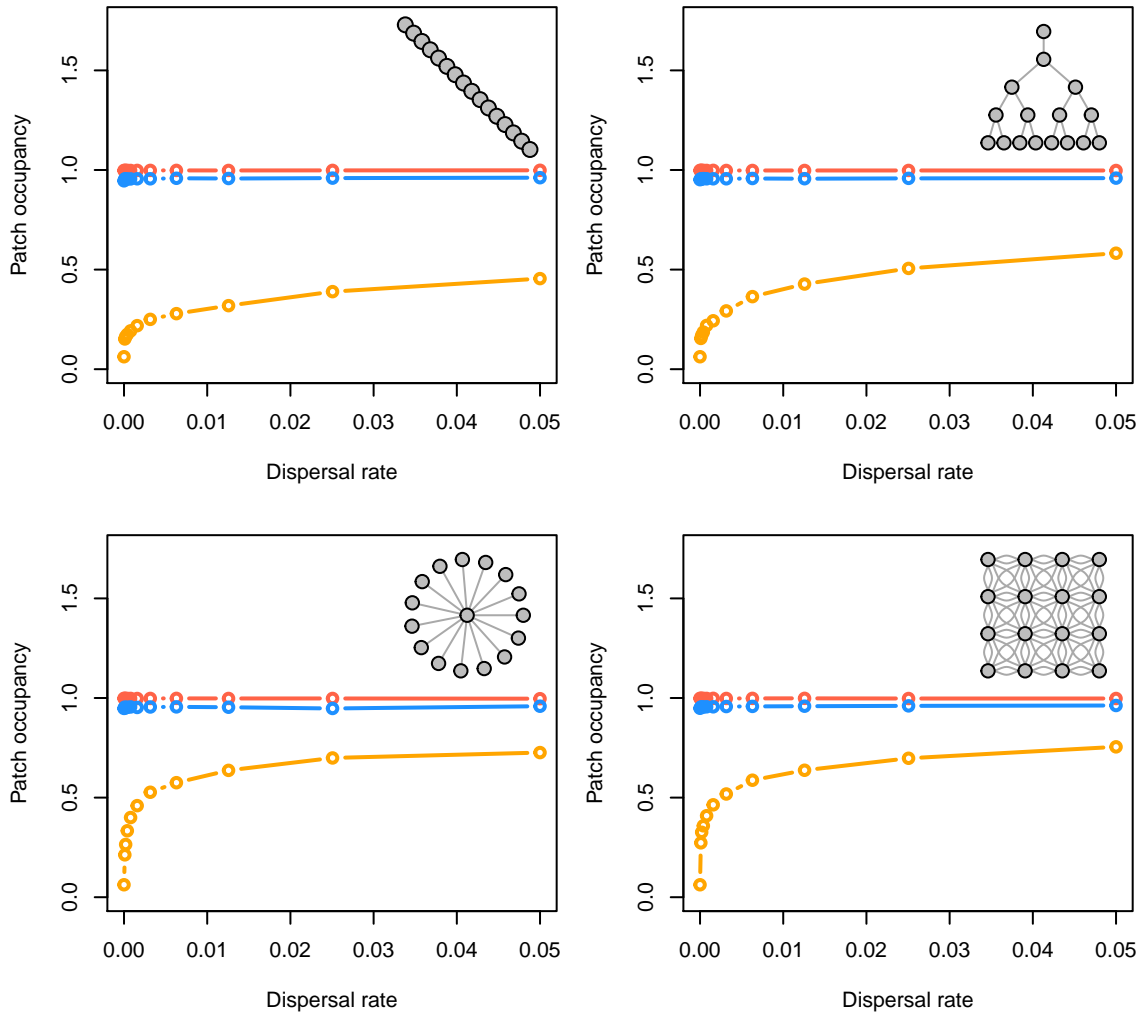

Figure S24: Patch occupancy after 25 years along dispersal, disturbance (red - uniform; blue - localized, random; orange - localized, extirpation), and network gradients with deterministic recruitment and homogeouns patches.

²⁸³ **Patch occupancy with variable patches**

²⁸⁴ Now, we illustrate how variable patch demography affects patch occupancy.
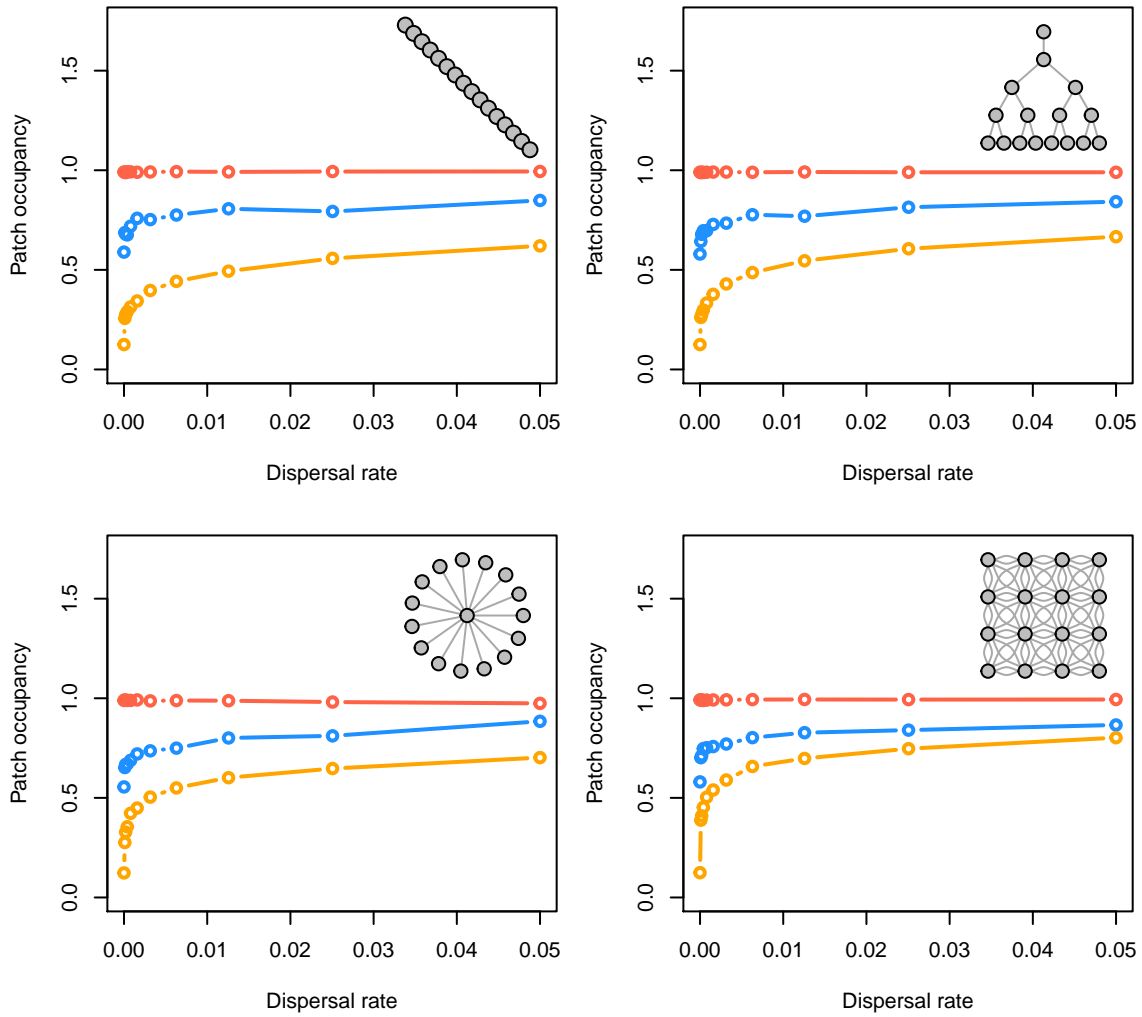

Figure S25: Patch occupancy after 25 years along dispersal, disturbance (red - uniform; blue - localized, random; orange - localized, extirpation), and network gradients with variable patches.

Patch occupancy with variable patches and stochasticity

Now, we illustrate how variable patch demography and stochastic recruitment affects long-term patch
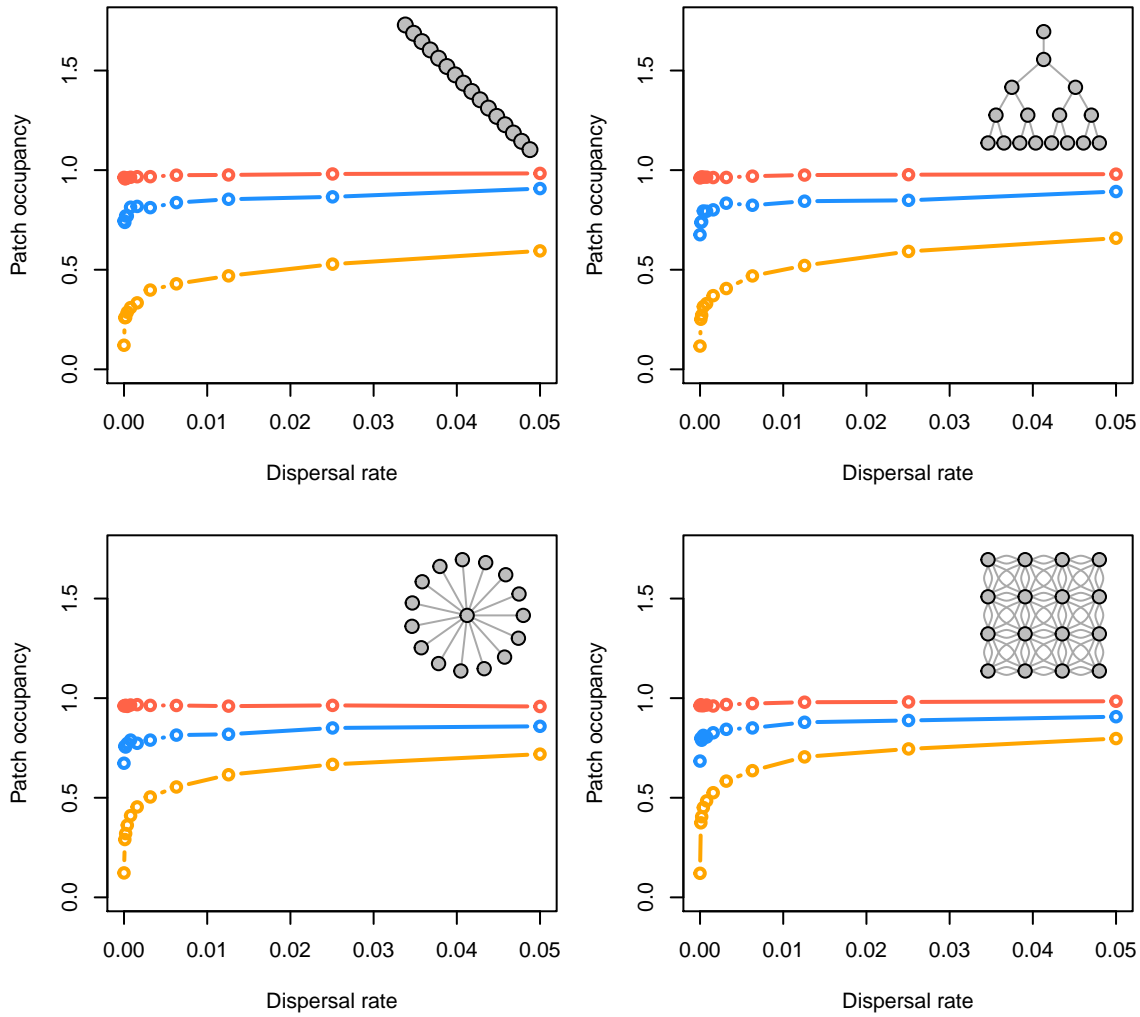occupancy.

Figure S26: Patch occupancy after 25 years along dispersal, disturbance (red - uniform; blue - localized, random; orange - localized, extirpation), and network gradients with variable patches and stochastic recruitment.

₂₈₈ **Patch occupancy with variable patches and spatio-temporally correlated stochasticity in**
₂₈₉ **recruitment**

₂₉₀ Now, we illustrate how variable patch demography and high spatial-temporal correlations in stochastic
₂₉₁ recrtuitment affects long-term patch occupancy.
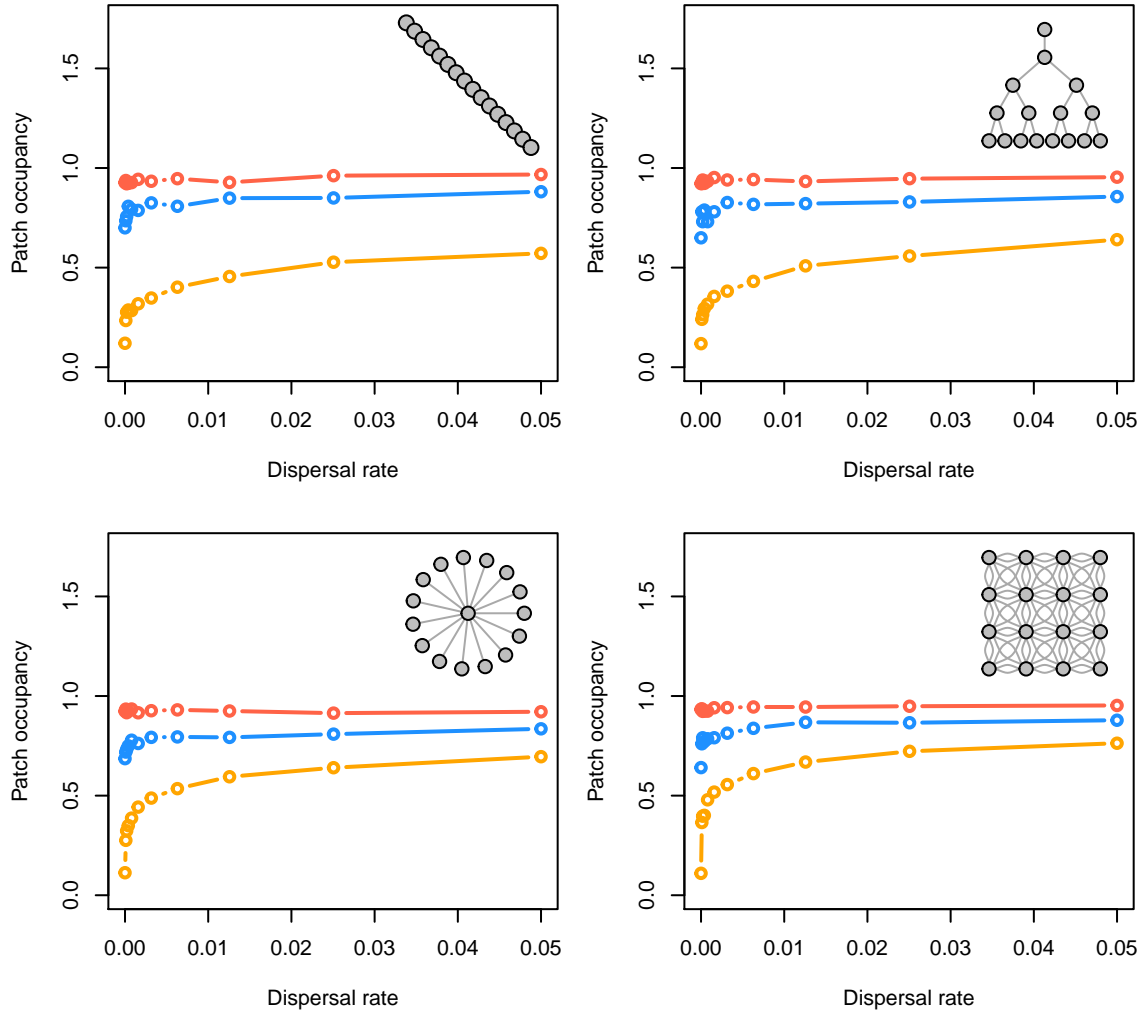

Figure S27: Patch occupancy after 25 years along dispersal, disturbance (red - uniform; blue - localized, random; orange - localized, extirpation), and network gradients with variable patches and spatial-temporal correlations in stochastic recruitment.

References

Anderson, S.C., Moore, J.W., McClure, M.M., Dulvy, N.K. & Cooper, A.B. (2015). Portfolio conservation of metapopulations under climate change. Ecological Applications 25 (2), 559-572. *Ecological Applications*, 25, 559–572.

Csardi, G. & Nepusz, T. (2006). The igraph software package for complex network research. *InterJournal*, Complex Systems, 1695.

Forrest, R.E., McAllister, M.K., Dorn, M.W., Martell, S.J. & Stanley, R.D. (2010). Hierarchical Bayesian estimation of recruitment parameters and reference points for Pacific rockfishes (Sebastes spp.) under alternative assumptions about the stock–recruit function. *Canadian Journal of Fisheries and Aquatic Sciences*, 67, 1611–1634.

Hanski, I. (1998). Metapopulation dynamics. *Nature*, 396, 41–49.

Yeakel, J.D., Moore, J.W., Guimarães, P.R. & Aguiar, M.A. de. (2014). Synchronisation and stability in river metapopulation networks. *Ecology Letters*, 17, 273–283.